

**ISCHEMIA INCREASES PROSTAGLANDIN H SYNTHASE-2 LEVELS  
IN THE RETINA AND BRAIN OF PIGLETS**

Ph.D. thesis

Rózsa Dégi, M.D.

Department of Ophthalmology  
Faculty of Medicine  
University of Szeged

2001.



## Table of contents

	Page
<b>List of abbreviations</b>	1.
<b>Summary</b>	2.
<b>Introduction</b>	4.
Characterization of arachidonic acid metabolism	5.
Nitric oxide in the nervous system	8.
Cerebral ischemia/ reperfusion	9.
Purposes of our study	10.
<b>Materials and methods</b>	11.
Surgical Procedure	11.
Experimental protocols	13.
Immunohistochemistry	13.
RN-ase protection assay	14.
Immunoblot analysis	15.
Statistical analysis	15.
<b>Results</b>	16.
COX-1	16.
COX-2	16.
Immunohistochemistry	16.
Rnase protection assay	32.
<b>Discussion</b>	36.
<b>Acknowledgements</b>	43.
<b>References</b>	44.
<b>Appendix</b>	50.

## List of abbreviations

7-NI =	7-nitroindazole	NO =	nitric oxide
AA =	arachidonic acid	NOS =	nitric oxide synthase
aCSF =	artificial cerebrospinal fluid	OCT =	optimal cutting
ATP =	adenosine triphosphate	transformer	
cDNA =	complementary deoxyribonucleic acid	OLM =	outer limiting membrane
COX =	cyclooxygenase	ONL =	outer nuclear layer
COX-1 =	cyclooxygenase-1	PL =	outer plexiform layer
COX-2 =	cyclooxygenase-2	P =	photoreceptor layer
DNA =	deoxyribonucleic acid	PBS =	phosphate buffer
eNOS =	endothelial nitric oxide synthase	saline	
G =	ganglion cells	PE =	pigment epithelium
GFAP =	glial fibrillary acidic protein	PGD <sub>2</sub> =	prostaglandin D <sub>2</sub>
INL =	inner nuclear layer	PGE <sub>2</sub> =	prostaglandin E <sub>2</sub>
ip =	intraperitoneal	PGF <sub>2α</sub> =	prostaglandin F <sub>2α</sub>
IPL =	inner plexiform layer	PG =	prostaglandin
IR =	immunoreactive	PGH <sub>2</sub> =	prostaglandin H <sub>2</sub>
IR-ity =	immunoreactivity	PGI <sub>2</sub> =	prostacyclin
iv =	intravenous	PL =	phospholipase
mRNA =	messenger ribonucleic acid	PLA <sub>2</sub> =	phospholipase A <sub>2</sub>
NFL =	nerve fiber layer	RN-ase =	ribonuclease
NGS =	normal goat serum	RPA =	ribonuclease
nNOS =	neuronal nitric oxide synthase	Tx =	protection assay
		TxA <sub>2</sub> =	thromboxane
			thromboxane A <sub>2</sub>

## Summary

Hypoxia/ischemia is a relatively common occurrence during the perinatal period. After successful resuscitation, an episode of hypoxia/ischemia can be followed by secondary insults, including seizure activity, intracranial hemorrhage, brain edema and visual impairment. The factors involved in the secondary progression of the neuronal injury have not been fully elucidated. There is increasing evidence that the enhanced release and action of excitatory amino acids, free radical-mediated reactions and intracellular  $\text{Ca}^{2+}$  accumulation are neurochemical processes that contribute to the progression of ischemic brain damage. Recent data indicate that the enzymes that synthesize the prostanoids and nitric oxide are important components of the formation of free radicals, and thereby play essential roles in the development of post-ischemic injuries.

The aim of our studies was to characterize the cellular localization and expression of cyclooxygenase (COX), the rate-limiting enzyme for prostanoid synthesis in the newborn brain. Using immunohistochemical techniques, we studied the distribution of prostaglandin H synthase -2 (cyclooxygenase-2 (COX-2)) and neuronal nitric oxide synthase (nNOS) in the piglet brain. We also examined the effects of ischemia and asphyxia on the levels of prostaglandin H synthase-1 (COX-1) and COX-2. However, the effects of ischemia on COX-2 mRNA and protein levels were investigated in the retina and in various regions of the brain.

Ischemia was induced by increasing intracranial pressure and lasted for 10 min. In some animals, indomethacin or 7-nitroindazole was administered prior to ischemia to block COX or nNOS, respectively. Tissues from the cerebral cortex, hippocampus, cerebellum and retina were removed and fixed and/or frozen after 1, 2, 4 and 8 hours of recovery from anoxic stress. Additionally, tissues were obtained from untreated animals or from time control animals. Levels of mRNA and proteins were determined by using a ribonuclease protection assay and an immunohistochemical approach, respectively.

In the tissues studied, only a few neurons were immunopositive for COX-1, and neither ischemia or asphyxia affected the COX-1 immunostaining at 8 hours after recovery. Likewise, the COX-1 mRNA level did not increase following anoxic stress. In contrast, substantial COX-2 immunoreactivity (COX-2 IR-ity) was present in the neurons and glial cells in the cerebral cortex, hippocampus, cerebellum and retina in the control animals. For

example, the neurons in cortical layers II/III, V and VI displayed very dense COX-2 IR-ity, whereas in the retina it was localized mainly to the outer limiting membrane and to the Müller cells.

Neurons, immunreactive for nNOS were limited in number and were widely dispersed across all layers of the cortex; they did not form a definable pattern. In the cerebellum, COX-2 IR-ity was heavily represented in the Bergman glia, and nNOS was detected in the basket cells. The levels of COX-2 mRNA were undetectable in the control animals, but exhibited dramatic increases in the brain and retina in the animals exposed to ischemia. The COX-2 mRNA level peaked by 2-4 hours after ischemia, and heightened COX-2 IR-ity was present at 6-8 hours: the COX-2 IR-ity was elevated in all layers of the retina, with the greatest increases in the photoreceptor layer. Interestingly, asphyxia did not enhance the COX-2 mRNA or immunostaining. Indomethacin pretreatment inhibited the increases in mRNA and protein for COX-2 after ischemia, while 7-nitroindazole had little effect on the increases in COX-2 immunoreactivity.

We have demonstrated that COX-2 is the predominant isoform present in the piglet brain and retina. COX-2 IR-ity is widely represented in the parietal and visual cortices, the hippocampus, the cerebellum and the retina. The distribution of nNOS is different from that of COX-2 in the neonatal brain. We have also shown that cerebral ischemia results in rapid increases in COX-2 IR-ity in all tissues investigated. Since COX and NOS-derived metabolites are involved in hypoxic/ischemic injuries, we conclude that elevated protein levels may be crucial factors in the development of secondary perinatal brain damage.

## Introduction

Disturbances in the fetal oxygen supply are common insults during the perinatal period. There has long been interest in determination of the relationship between an insufficient exchange of respiratory gases, an inappropriate blood supply to the brain in perinatal life and their neuropathologic manifestations in surviving children (Vannucci, 1993). Extensive research conducted in the past several years has led to a better understanding of the mechanisms involved in perinatal hypoxic/ischemic brain injury. These studies have revealed that different pathogenetic mechanisms, such as a decreased blood flow autoregulation, an altered cerebral metabolism, thrombosis, hemorrhage, the accumulation of toxic metabolites such as glutamate, an impaired intracellular  $\text{Ca}^{2+}$  turnover, the release of interleukins and prostaglandins (PG-s), Fe accumulation and the overproduction of free radicals, are the major components of the neuronal impairment (Berger and Garnier, 2000). It has also been clarified that the brain tissue injuries observed following ischemia have two major phases (Vannucci, 1993; Volpe, 1994). In the first, acute phase, the inappropriate oxygen supply has a direct effect on the cellular functions. Minutes of severe ischemia affect specific populations of neurons where irreversible cellular injury is initiated (Siesjö and Siesjö, 1996). Clinical and experimental data have also revealed that severe perinatal asphyxial injury is associated with a latent phase after reperfusion (Vannucci, 1993; Volpe, 1994). The cerebral energy metabolism recovers initially, but the EEG remains suppressed (Williams et al, 1992). This period is followed by a secondary phase with seizures, cytotoxic edema, the accumulation of cytotoxins, and cerebral energy failure from 6 to 15 hours after birth. At this time, additional cell injuries can occur (Berger and Garnier, 1999).

Studies from our own laboratories and other have shown that hypoxia, asphyxia and cerebral ischemia are associated with a prolonged cerebrovascular dysfunction (Bari et al., 1996a,b,c). There is a strong suggestion that an incongruity between the cerebral oxygen supply and demand may be involved in the mechanisms leading to secondary brain injuries (Hossmann, 1999).

Like other parts of the central nervous system, the retina is vulnerable to ischemia/reperfusion injury (Bazan, 1989; Bazan and Allan, 1997). The principal damage to the retina is related to the direct effects of energy failure. Similarly as in the other brain regions, a delay in the onset of neuronal cell death also occurs following ischemia in the retina. Most studies on the

postischemic retina have reported that cell death is most pronounced in the inner retina (Bazan, 1989; Hardy et al., 2000). Although the precise mechanisms of ischemia-induced neuronal death are unknown, excitotoxicity triggered by the overactivation of glutamate receptors is considered to be a central component of postischemic necrosis in the nervous tissues, including the retina (Hardy et al., 2000).

Ischemia is known to disrupt the cellular energy state, to acidify intra- and extracellular fluids and to cause the loss of ionic homeostasis. The primary event in all ischemic conditions is a deficient delivery of oxygen to the mitochondria, leading to a compromised production of ATP and a deranged cellular energy metabolism. Energy failure is accompanied by a massive release of  $K^+$  from the cells, and by the uptake of  $Ca^{2+}$ ,  $Na^{2+}$  and  $Cl^-$  (Hansen, 1985). Cerebral ischemia disrupts the tightly regulated events that control the production and accumulation of lipid messengers, such as free arachidonic acid (AA), diacylglycerol and platelet activating factor under physiological conditions. A rapid activation of phospholipases (PL-s), and particularly of PL A<sub>2</sub>, occurs at the onset of cerebral ischemia. Whereas pathways leading to PLA<sub>2</sub> activation/release are part of the normal neuronal function, a number of data indicate that an overproduction of PLA<sub>2</sub>-derived lipid derivatives is involved in neuronal damage (Chemtob et al, 1993; Hall, 1997). In recent years, it has become evident that, even after the successful termination of cerebral ischemia, additional cellular damage occurs in the reperfusion period. The contributors to tissue damage include oxygen free radicals and  $H_2O_2$ , which have diverse, detrimental effects on the cellular functions (Floyd, 1997). Increasing evidence suggests that one of the most important components of ischemic injuries is the damage to the membrane lipids.

### **Characterization of the AA metabolism**

AA products such as prostaglandins, Tx-s, and 15-hydroxyeicosatetraenoic acids are collectively referred to as eicosanoids. These products are involved in various physiological and pathological processes, including inflammation, and the modulation of immune responses or pain sensation. The regulation of eicosanoid production has become an area of intense study because these fatty acid metabolites affect multiple signaling pathways that modulate a wide range of cellular functions. The two major determinants of eicosanoid production are the availability of substrates and the presence of synthetic enzymes. The biosynthetic pathway for eicosanoids has multiple steps that are possible sites of regulation. Several PL-s, which liberate AA from membrane phospholipids have been characterized. The PL-s have important

regulatory functions in eicosanoid production. AA can be metabolized in three main pathways via the actions of oxidative enzymes such as cyclooxygenases (COX-s), lipoxygenases and cytochrome P-450 monooxygenases (Shimizu and Wolfe, 1990).

The relative levels of various eicosanoids are determined by different synthetic enzymes that are under genetic control and are specific for the cell type and the physiological conditions. The clearest example is the predominant production of prostacyclin by endothelial cells and of TXA<sub>2</sub> by platelets from the same precursor following the initial conversion of AA (Vane and Botting, 1995).

The various PG-s and Tx-s produced by COX are often collectively referred to as prostanoids. During the prostanoid production, the free AA is converted to PGG<sub>2</sub> /H<sub>2</sub> (PGH<sub>2</sub>) via prostaglandin G/H synthase, which is identical to COX (Busija, 1997). Two isoforms of COX have been described. COX-1 appears to be the constitutive form. COX-1 mRNA and protein are present at relatively stable levels in many tissues, but the prostanoid production of these tissues is variable. Recently a second, inducible form of COX (COX-2) has been identified. COX-2 expression is induced by a wide range of extra- and intracellular stimuli, including interleukin-1, tumor necrosis factor or synaptic activity (DeWitt, 1991; Wu, 1996; Breder, 1997). The transcription of COX-2 mRNA does not require new protein synthesis; therefore, it is an immediate early gene (O'Banion et al., 1992). In addition to its expression at sites of inflammation, COX-2 is also expressed constitutively in a number of tissues, including the kidney and the brain. Detailed studies on adult animals have demonstrated that COX-1 is expressed in almost all structures in the central nervous system. In contrast, COX-2 is mainly expressed in the cortex, the hypothalamus and the hippocampus (Breder et al., 1995). The brain COX-2 is identical to the non-nervous system COX-2 (Yamagata et al., 1993). It is not yet clear what the specific roles of the two isoforms are in the central nervous system. However, it has been known for some time that prostanoids modulate activities such as thermoregulation and sleep (Stitt, 1986; Hayaishi, 1988). Prostanoids (PGD<sub>2</sub>, PGE<sub>2</sub>, PGF<sub>2a</sub>, PGI<sub>2</sub> and TXA<sub>2</sub>) are produced from PGH<sub>2</sub> via specific enzymes. The regulation of COX-1 and COX-2 expression is therefore a key step in prostanoid production (Smith, 1992).

PG-s act as modulators in several neurological and cerebral hemodynamic functions (Busija, 1996; 1997). During the perinatal period, the concentrations of PG-s in the blood and brain in the newborn are higher than those in the normal adult. It has been shown that the COX-2 expression is increased in the brain cortex and periventricular white matter of the newborn



and is the main source of high PG-s levels, such that the COX-2 activity accounts for ~80% of the total COX activity in the perinatal brain, whereas in the adult it is responsible for <10% of the total COX activity (Dumont et al., 1998). The COX-1 expression in brain is unaltered during this developmental period. The prostanoids appear to play a particularly important role in the regulation of cerebral and the retinal circulation during the perinatal period (Zhu et al, 1998). In this early stage of extra-uterine life, COX products have diverse effects on the cerebrovascular responses to a number of neurotransmitters (Busija, 1996). Inhibitors of COX activity reduce the basal cerebral blood flow, and minimize the dilator responses to arterial hypercapnia and hypotension.

Neuronal excitation and an increased intracellular  $\text{Ca}^{2+}$  level, two stimuli that induce the expression of COX-2, are also important in the pathophysiology of neuronal death in ischemia and a variety of neurodegenerative diseases (Rothman and Olney, 1986; Choi, 1997).

The retina exhibits COX activity and synthesizes all major PG-s (Goh et al., 1987, Hardy et al, 2000). PG synthesis in the retina can be activated by various conditions, such as exposure to high-intensity visible light (Birkle et al., 1989; Hanna et al, 1997). Further,  $\text{PGE}_2$  and  $\text{PGF}_{2\alpha}$  receptors are located on the retinal blood vessels, whereas  $\text{PGE}_2$  and  $\text{PGD}_2$  binding sites are present on various cell types, including photoreceptors, and bipolar, horizontal, ganglion and Müller cells (Matsuo et al., 1992; Kulkami and Payne, 1997; Hardy et al., 1998). AA metabolites, possibly including prostanoids, also participate in the control of the retinal blood flow during hypo- and hypertension, but do not seem to control the basal circulation (Chemtob et al., 1991; Abran et al., 1994; 1995). Similarly, COX-derived metabolites would be expected to participate in the neuronal and vascular responses in the visual cortex (Yamagata et al., 1993).

In addition to the production of prostanoids, the conversion of AA results in the simultaneous production of the superoxide anion. This can have a particularly important role in the brain and retinal pathology during recovery from anoxic stresses such as ischemia or asphyxia, when large amounts of radicals are formed (al-Zadjali et al., 1994; Hardy et al., 1994; 2000). In the selectively vulnerable neurons, radical damage during reperfusion is aggravated by further factors, such as their deficiency in glutathione peroxidase or their high Fe content.

It is unclear whether the levels of constitutively expressed COX-2 are increased in the nonvascular tissues in the neonatal brain following anoxic stress. Augmented levels of the COX isoforms in the neurons and glial cells following anoxic stress might lead to an enhanced capability for the production of the superoxide anion during delayed, secondary insults, and thereby promote additional neuronal injury. Furthermore, recent data support the hypothesis that COX-2 activity leads directly to neuronal injury (Hara et al., 1998).

#### **Nitric oxide in the nervous system of the neonate**

The three isoforms of nitric oxide synthase (NOS) include the  $\text{Ca}^{2+}$ -independent isoform, which is expressed mainly in the macrophages, and the  $\text{Ca}^{2+}$ -dependent isoforms, present in the endothelial cells (eNOS) and the neuronal tissues (nNOS). Nitric oxide (NO), formed via the nNOS, acts as a signal for the development and shaping of neuronal cells and their activity (Szabó, 1996), and also for the control of the blood supply to the brain in response to metabolic demands. More than 95% of all NOS activity in the brain is attributed to nNOS (Szabó, 1996).

NOS displays a precise pattern of increased activity in the nervous system during the perinatal period in various species, including rodents, pigs, cats and humans. These developmental changes in NOS activity immediately precede a period of maximal synaptogenesis, in which it has been implicated (Mishra and Delivoria-Papadopoulos, 1999). Similar functions have been ascribed to COX-2. The mechanisms regulating this high NOS activity in the perinatal period are not well understood. Although a role has been suggested for estrogens, this contribution is only partial. A role for PG-s in regulating NOS activity under certain conditions has been proposed. It has been reported that COX inhibitors markedly inhibit NO production in the rat alveolar macrophages. This fact has led to the suggestion that the inhibition of PG synthesis results in an inhibition of NOS gene expression and in turn in a decreased NO synthesis. There is also evidence that the constitutive NOS (eNOS and nNOS) can potentially be induced by the PG-s (Salvemini et al., 1993). Furthermore, the suggested role of estrogens in partially governing the NOS activity may be partly mediated by the PG-s, since estradiol can stimulate PG synthesis (MacRitchie et al., 1997).

As NOS has the potential of being induced by the PG-s (Salvemini et al., 1993), and both the PG levels and the NOS activity have been found to be high in the brain tissue of the perinate

(Mishra and Delivoria-Papadopoulos, 1999), a precise interplay can be hypothesized between the PG-s and nNOS in the brain in the newborn can be.

### **Cerebral ischemia/reperfusion**

Cerebral hypoxia/ischemia during the perinatal period in humans is often followed by extensive brain damage. As in adults, the developing brain is subjected to ischemia-induced injury, such as global necrosis, focal infarction, selective neuronal necrosis, and border zone infarction (i.e. in regions at the edge of the terminal blood supply). The major observations during investigations of brain injury by ischemia and reperfusion were as follows:

1. morphologic studies revealed that most of the structural damage occurs during reperfusion;
2. progressive hypoperfusion of the brain occurs during reperfusion; and
3. there is a prolonged suppression of protein synthesis (Berger and Garnier, 2000).

Although most of the phenomena observed following brain ischemia have been known for decades, the understanding of the mechanisms involved in the damage and in the possible repair remains inadequate. The fact that cellular division and migration, neurite outgrowth, myelination and synapse formation occur during the perinatal period makes the developing brain particularly susceptible to anoxic stress. The high-energy metabolism in the brain is fully dependent on the blood supply. During ischemia, a very rapid rundown of ATP occurs, which is accompanied by ionic shifts and  $\text{Ca}^{2+}$ -mediated enzymatic lipolysis. In the lack of a blood/oxygen supply, the brain ATP levels approach zero within minutes. Reperfusion results in oxidative metabolism of the AA released during ischemia, with the consequent generation of the superoxide radical, the reduction and release of stored ions, and the exacerbation of membrane damage by lipid peroxidation. Since cellular damage is consistently observed in the cerebral cortex, hippocampus, and cerebellum, these brain regions are considered to be particularly vulnerable to anoxic stress (Vannucci, 1995).

The molecular basis of the selective vulnerability of various brain structures, or even of various cell types within one region, is still an enigma. Depending on the severity of the damage induced by the ischemic insult and the properties of the afflicted neurons, cell death may occur rapidly, during a few hours, or slowly, over several days or months. Studies on overall postischemic protein synthesis activity demonstrate a general translation deficit. The lethally damaged neurons exhibit an irreversible translation block, whereas the protein synthesis in the surviving neuronal populations finally recovers completely. There is evidence

that the extent and duration of protein synthesis inhibition vary in the different regions of the brain. The regional differences in the prolonged inhibition of protein synthesis are correlated with morphological evidence of cellular injury (Wieloch et al., 1997).

Even though the protein synthesis in general appears to be suppressed, an increased synthesis of specific proteins in the early phase of ischemia/reperfusion has been reported in both adults and neonates. Functional analysis of the early-expressed proteins has shown that some of them may be beneficial for cell survival (Koistinaho and Hökfelt, 1997). However, the early appearance of other enzymes could be detrimental (Gass et al., 1997). The effect of ischemia/reperfusion on protein synthesis should therefore be considered an important step in the understanding of the development of cerebral injury after anoxic stress.

To replicate the features of human ischemic injuries, various animal models have been investigated. The best animal model of neonatal hypoxic/ischemic brain injury is the one that most closely approximates to the damage found in human infants. However, both clinically and in animal models, the type of damage observed will depend on the maturity of the brain. Several species, including mice, rats, guinea pigs, rabbits, cats, dogs, piglets, sheep and monkeys, are used for studies of neonatal brain injuries (Raju, 1992). Detailed direct comparisons between species indicate that, during the first 2 weeks postpartum, the piglet brain displays developmental and morphological similarities with that of human babies. (Buckley, 1986). The use of piglets to study the effects of cerebral ischemia/reperfusion therefore offers several advantages. In addition, since this species is widely used for investigations of cerebrovascular function, a considerable amount of information is available regarding the piglet physiology, pharmacology and neural electrophysiology.

**The purposes of our studies were as follows:**

1. To characterize the distributions of COX-2 and nNOS in the neonatal brain. We focused on three particularly interesting regions: the cerebral cortex, the hippocampus and the cerebellum. These areas were chosen because they represent different stages of development in the neonatal brain and because of their susceptibility to damage after hypoxic/anoxic stress (Vannucci, 1993).
2. To characterize the effects of anoxic stress on the brain levels of COX-1 and COX-2 and to test the hypothesis that anoxic stress may increase the brain levels of COX-2, but not COX-1. We focused on the responses in the parietal and visual cortices and the

hippocampus. We also examined the effects of two different kinds of anoxic stress, 10 minutes of total ischemia or 10 minutes of whole-body asphyxia.

3. To examine the regulation of COX-2 in the retina. We tested the hypotheses that COX-2 is constitutively expressed in the retina, and that transient cerebral ischemia causes rapid increases in COX-2 levels.
4. To examine the effects of indomethacin pretreatment on the increases in COX-2 following ischemia. Previous studies have shown that indomethacin pretreatment blocks superoxide anion production (Armstead et. al., 1988; 1989; Pourcyrous et al., 1993) and preserves the cerebrovascular responsiveness (Bari et al., 1996a, b) following cerebral ischemia.
5. To characterize the effects of the inhibition of nNOS by 7-nitroindazole (7-NI) on the increases in COX-2 following ischemia. NO from nNOS has been suggested as a mediator of neuronal damage following ischemia (Huang et al., 1994; Zhang et al., 1996), but the role of nNOS in regulating the production of COX in the brain has not been examined.

### **Materials and methods**

#### **Surgical procedure**

In this study, 1-7- day-old piglets of either sex with body weights of 0.9-1.4 kg were used. Anesthesia was induced with sodium thiopental (30-40 mg/kg), followed by an intravenous (iv) injection of  $\alpha$ -chloralose (75 mg/kg). Supplemental doses of  $\alpha$ -chloralose were given as needed to maintain a stable level of anesthesia. The animals were intubated via tracheotomy and artificially ventilated with room air. The ventilation rate (~ 20 breaths/min) and tidal volume (~ 20 ml/kg) were adjusted to maintain the blood pH and gas values within the physiological ranges. In our study, these animals had baseline values within the normal limits for arterial pH (7.45 $\pm$ 0.04), pCO<sub>2</sub> (32 $\pm$ 4 mmHg), and pO<sub>2</sub> (95 $\pm$ 4 mmHg) (n=69).

Body temperature was maintained at 37-38 °C by a water- circulating heating pad. Systemic arterial blood pressure was recorded via a catheter placed into the right femoral artery, which was connected to a pressure transducer. The right femoral vein was catheterized for the administration of drugs and fluids. The heads of the piglets were fixed in a stereotaxic frame. The scalp was incised and the connective tissue over the parietal bone was removed. A craniotomy for a stainless steel-glass cranial window 19mm in diameter was made in the left parietal bone approximately 10mm rostral to the coronal suture. The dura was exposed, cut

and reflected over the skull. A cranial window with three needle ports was placed into the craniotomy, sealed with bone wax and cemented with cyanoacrylate ester and dental acrylic. The closed window was filled with artificial cerebrospinal fluid (aCSF) warmed to 37 °C and equilibrated with 6% O<sub>2</sub> and 6.5% CO<sub>2</sub> in N<sub>2</sub>. The aCSF consisted of KCl 2.9, MgCl<sub>2</sub> 1.4, CaCl<sub>2</sub> 1.2, NaCl 132, NaHCO<sub>3</sub> 24.6, urea 6.7 and glucose 3.7 mmol/L. The diameters of the pial arterioles were measured by using a microscope (Wild M36, Switzerland) equipped with a video camera (Panasonic, Japan) and a video micro scaler (IV-550, For-A Co. Newton, MA). Following the surgical procedure, the cranial window was gently infused several times, with aCSF until a stable baseline was obtained.

#### *Hypoxic models used*

Asphyxia was achieved by turning off the ventilator and clamping the endotracheal tube. After 5 or 10 minutes of asphyxia, the tubing was unclasped and the animals were reventilated. During resuscitation, iv epinephrine was given as needed to prevent asystole and 3 ml/kg 4.2% NaHCO<sub>3</sub> solution was administered to counteract systemic acidosis.

Cerebral ischemia-reperfusion injury was produced by elevation of the intracranial pressure to above the perfusion pressure, which was estimated via the arterial blood pressure. During the surgical procedure, a hollow brass bolt was placed in the left cranium without damaging the dura. This bolt allowed the infusion of aCSF into the cranium, resulting in an increased intracranial pressure. During ischemia, venous blood was withdrawn as necessary to maintain the mean arterial pressure near normal. This was important to counteract the intense Cushing response. During ischemia, a complete cessation of blood flow to the cortex was evaluated by intravital microscopy. Lack of blood flow to the various regions other than the pial surface of the brain was verified by using a microsphere technique. During this procedure, colored microspheres 15 µm in diameter were injected into the left ventricle of the heart. A reference blood sample was collected from the femoral artery. Because of their rigidity, these microspheres were entrapped in the microcirculatory network, indicating the intensity of tissue perfusion. Analysis of the number of microspheres detected in each region of the brain and the retina indicated that ischemia was widespread and total. As an example, prior to ischemia there were 216 ± 27 microspheres/g in the parietal cortex (n=4), whereas in the retina there were 176 ± 37 microspheres/g (n=4). During ischemia, the blood flow ceased in all the tissue samples investigated, as indicated by the lack of spheres detected (<1

ml/min/100g). After 10 minutes of ischemia the infusion tube was clamped and the intracranial pressure was allowed to normalize.

### **Experimental protocols**

Anesthetized, instrumented piglets were divided into three groups: the asphyxia group (n=12), the ischemia group (n=39), and the time control group (n=35). Some animals received indomethacin (5 mg/kg, iv) (n=7) or 7-NI (50 mg/kg, ip) (n=12) prior to ischemia.

Indomethacin is an effective blocker of COX in the cerebral tissues of piglets (Armstead et al., 1988; Pouryrouz et al., 1993, Bari et al., 1996a), while 7-NI is an effective blocker of nNOS in piglets (Bari et al., 1996b). The time control animals were treated in the same way as the other two groups, except that they were not exposed to asphyxia or ischemia. Animals were killed under anesthesia with KCl at 1, 2, 4, 6, 8 and 12 hours after ischemia or asphyxia. Tissue samples were also obtained from untreated, euthanized (sodium thiopental, 150 mg/kg, ip) control animals (n=10).

The brain was removed quickly and samples of the cerebral cortex, cerebellum, hippocampus and retina were immersion-fixed in 10% neutral, buffered formalin for 15-24 hours or frozen by immersion in 2-methylbutane at -70 °C. Frozen samples were stored at -60 °C. Samples from the thalamus and the superior colliculus were also frozen.

### **Immunohistochemistry**

The eyes were opened at the corneal-scleral border with a sharp blade and placed in neutral buffered formalin. After fixation, the neural retina was removed with fine forceps, washed thoroughly in 10 mmol/L phosphate buffer/0.9% saline, pH 7.4 (PBS), embedded in optimal cutting transformer (OCT) and stored at -60 °C until cryostat sectioning. Brain tissues were immersion-fixed overnight in the same fixative, washed in PBS and stored at 4°C until vibratome-sectioned.

Sections of brain tissues (50 µm) and retina (8 µm) were stained free-floating by a three- step immunoperoxidase method.

After washing in PBS, 50 µm vibratome sections were cut and collected in PBS containing 0.1 mg/l of thimerosal. All washes and solutions were made in PBS unless otherwise stated. The sections were incubated in 50 mmol/L NH<sub>4</sub>Cl for 1 hour, washed, and incubated in 0.3% Triton X-100 for another hour. After washing, the sections were blocked in 10% normal goat serum (NGS)/0.1% Tween 20 (NGS-T) for 4 hours. Antibodies specific for COX-1 (Dr.

Steve Prescott, Salt Lake City, UT) and COX-2 (Dr. A. W. Ford-Hutchinson, Merck Fross Center for Therapeutic Research, Pointe Claire, Quebec, Canada or PG 26, Oxford, Oxford, MI) were diluted 1:2000 and 1:10,000, respectively, in NGS-T and incubated with brain sections overnight at room temperature. The use of either COX-2 antibody yielded virtually identical results. For consistency, all of the photomicrographs of COX-2 immunostaining reflect the use of the antibody from Dr. Ford-Hutchinson. After the rinsing of sections in NGS, endogenous peroxidase was blocked by incubating the sections in 3% H<sub>2</sub>O<sub>2</sub>/10% methanol for 30 minutes. After washing, anti-COX-2 sections were incubated for 2 hours in biotinylated goat anti-rabbit IgG (Vector, Burlingame, CA), diluted 1:1000 in 2% NGS. Anti-COX-1 sections were treated similarly and were incubated for 2 hours in biotinylated goat anti-mouse IgG (Vector), which was diluted 1:1,000 in 2% NGS for 2 hours. Subsequently, sections were washed and reacted with Vector ABC reagent (Vector) for 30 minutes, washed again, and reacted with diaminobenzidine. Stained sections were mounted on slides, dried, and covered with cover glass. The specificity of immunostaining was established by using several approaches. Sections were incubated as described, but without antibody (secondary antisera only) or with normal rabbit serum instead of primary antibody. Further the COX-2 antibody was preadsorbed with 580 units of purified COX-2 (Cayman Chemical Co., Ann Arbor, MI) prior to incubation with sections.

We used two approaches to characterize the cellular patterns in the areas examined. First, the general cellular morphology was assessed by cresyl violet staining. Second, immunostaining was performed with an antibody (dilution 1:50,000) against glial fibrillary acidic protein (GFAP), using the same procedures as described above.

Sections were visualized and photographed with a Zeiss Axioskop microscope (Jena, Germany). Figures were created with Adobe Photoshop (San Jose, CA) software from original 35mm color slides and negatives, and were printed with a Fuji-x Pictograph 3000 digital printer (Encino, CA). Scanning contrast and intensity were altered only in order to replicate the original images. The color images were converted to the gray scale by using filters as necessary, formatted to plate form and labeled.

#### **RNase protection assay (RPA)**

Total RNA was extracted in homogenization buffer (4 mol/L guanidium isocyanate, 25 mmol/L sodium acetate, 0.1 mol/L  $\beta$ -mercaptoethanol). After sonication, the homogenates

were transferred to phase-lock gel tubes (5-prime-3-prime, Boulder, CO). 100  $\mu$ l of 2 mol/L sodium acetate was then added to each sample, followed by 1 ml of H<sub>2</sub>O-saturated phenol. After thorough mixing, 300  $\mu$ l of chloroform: isoamyl alcohol (49:1) was added, and the solution was incubated on ice for 10 minutes before centrifugation at 6,000 rpm for 5 minutes. The supernatants were transferred to fresh tubes. After the addition of 1 ml of isopropanol, the samples were incubated at room temperature for 30 minutes and centrifuged at 12,000 rpm for 25 minutes. The resulting pellets were washed with 100% ethanol and re-dissolved in ultrapure water before storage at -60 °C. The integrity of the RNA was determined by resolution in an 1% agarose gel, and RNA aliquots were quantified spectrophotometrically.

RPA-s were carried out on 25  $\mu$ g of total RNA from each sample, using RPA II kits (Ambion, Austin, TX). <sup>32</sup>P-labeled sense and antisense probes were generated for COX-1 and COX-2 by using MaxiScript kits (Ambion) after the linearization of plasmids containing fragments of DNA for porcine COX-1 and COX-2 (Dr. Sylvain Chemtob, Research Centre Of St. Justine Hospital, Montreal, Canada). The protected fragments were resolved on 6% urea/acrylamide gel and autoradiographed using hyperfilm (Amersham, Arlington Heights, IL).

### Immunoblot analysis

Protein was extracted from frozen retinas in boiling lysis buffer (10 mmol/L Tris and 1% SDS). The samples were sonicated, heated at 95 °C for 5 minutes, and centrifuged for 15 minutes at 12,000 rpm at 4 °C. An aliquot of the supernatant was removed for protein concentration determination. After the addition of an equal volume of sample buffer (100 mmol/L Tris, pH 6.8; 42% glycerol; 5% bromophenol blue; and 1% SDS) to each sample, the protein was separated on a 4-20% gradient of mini gel (Bio-Rad, NY) and transferred to nitrocellulose. After nonspecific protein binding was blocked by incubating the blot in 5% milk, primary antibody against COX-2 (1:1000) was applied, followed by horseradish peroxidase-conjugated secondary antibody (1:10,000) (goat anti-rabbit, Jackson Immunoresearch Labs, PA). Electrochemiluminescence was utilized to visualize the bands. Molecular weight markers were also run.

### Statistical analysis

All numerical values are reported as means  $\pm$  SD.



## Results

### A. COX-1

Very little immunoreactivity (IR-ity) for COX-1 was present in the cerebral cortex (Fig. 1A,C) or hippocampus (not shown) samples from the time control or untreated animals. Moreover, mRNA for COX-1, though detectable, was relatively low in the time control animals (Fig. 1D). Detection of mRNA for COX-1 required longer times of incubation of gels with film than for COX-2 (compare sample versus probe lanes for COX-1 in Fig. 1D with those for COX-2 in Figs 9 and 13-15). Further, the IR-ity (Fig. 1B) and mRNA levels (Fig. 1D) for COX-1 did not increase following anoxic stress in any region examined.

### B. COX-2

#### *Immunohistochemistry*

##### Control conditions

###### a. Cerebral cortex

The immunolocalization of COX-2 in the cerebral cortex after 8 hours in the time control piglets revealed widespread staining in virtually all cortical layers, but IR-ity was readily evident in layers II/III, V and VI (Fig. 2A,D). The COX-2 IR-ity throughout the layers was moderate and uniform in intensity; it was most evident in the pyramidal neurons of layer V (Fig. 2D). Little or no cell-specific IR-ity was observed when sections were incubated with secondary antibody only, normal rabbit serum instead of primary antibody, or COX-2 antibody which had been preadsorbed with purified COX-2 (Fig. 2F). The pattern of COX-2 IR-ity in the parietal cortex from the time control animals was nearly identical to that in the untreated animals (not shown).

###### b. Hippocampus

While COX-2 IR-ity was evident in various regions, an aggregate of subgranular, polymorphic neurons in the superficial hilus of the dentate gyrus consistently displayed intense immunostaining in the time control samples (Fig. 3A). Limited COX-2 IR-ity was also observed in the field CA3 pyramidal cells (Fig. 3B), although the intensity was more variable than that detected in the dentate gyrus. Uniform and widespread COX-2 IR-ity was also observed in small stellate cells in the molecular layer of the hippocampus and bordering

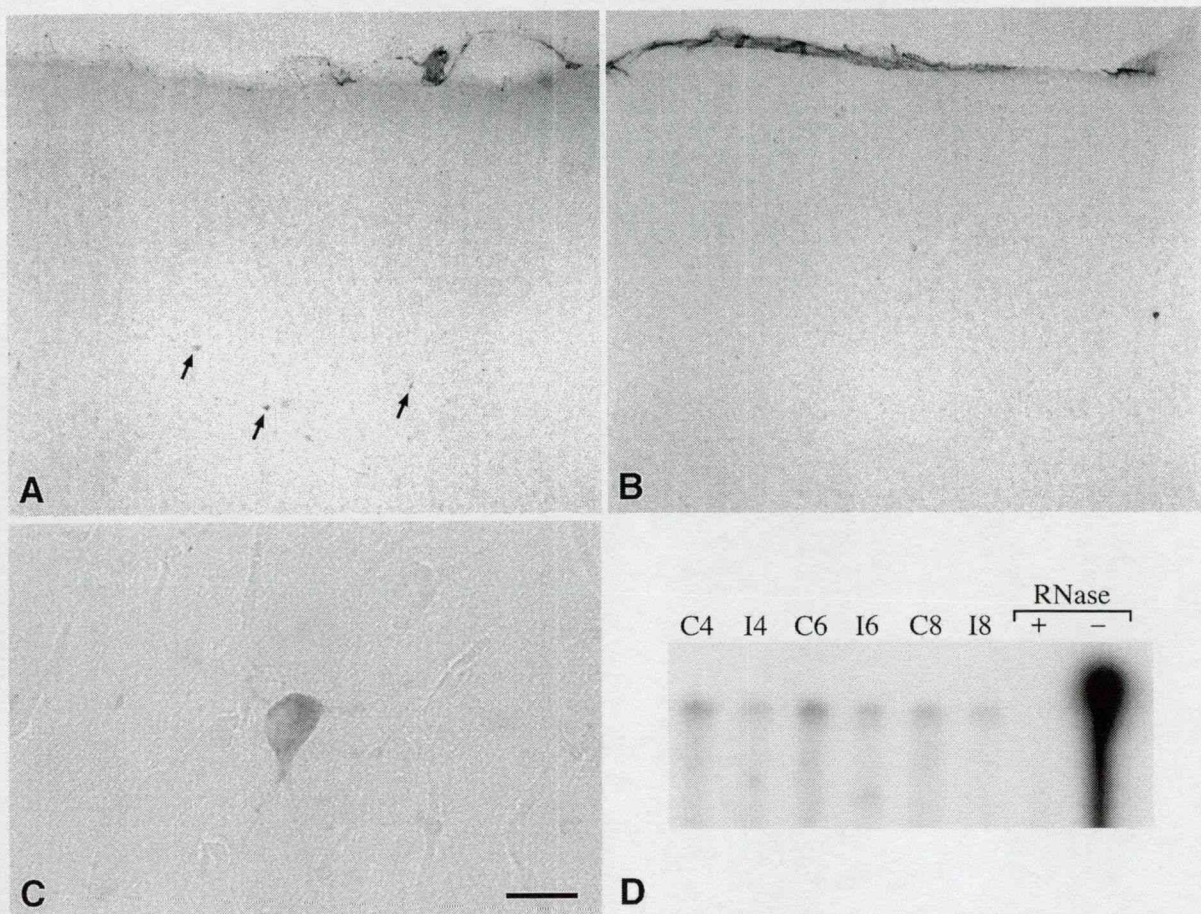


**Figure 1.**

COX-1 representation in cerebral cortex. A) Only a few neurons (arrows) were immunopositive for COX-1 in a 8 hour time control animal. B) No significant increase in COX-1 immunoreactivity was detected in cortex 8 hours after ischemia. C) Higher magnification of one of the neurons shown in A. COX-1 immunoreactivity was localized to the cell body with no immunostaining extending into the processes. D) RNase Protection Assay showed detectable COX-1 mRNA in time control animals, but no increase in mRNA following ischemia. Long X-ray exposure times relative to those for COX-2 blots (see next figure) were necessary to detect COX-1 mRNA in piglet cortex. The 4, 6, and 8 hr time control lanes are indicated as C4, C6, and C8, respectively. Likewise, 4, 6, and 8 hrs after ischemia are indicated as I4, I6, and I8, respectively. Unprotected probe digested with RNase is shown in '+' lane, while the unhybridized, undigested probe is shown in the '-' lane. Note that the unprotected band shown in the last lane of the hippocampus and cerebellum blots runs at 293 bp and the hybridized bands migrate at 235 bp. Bar represents 200  $\mu$ m in panels A and B and 25  $\mu$ m in panel C.

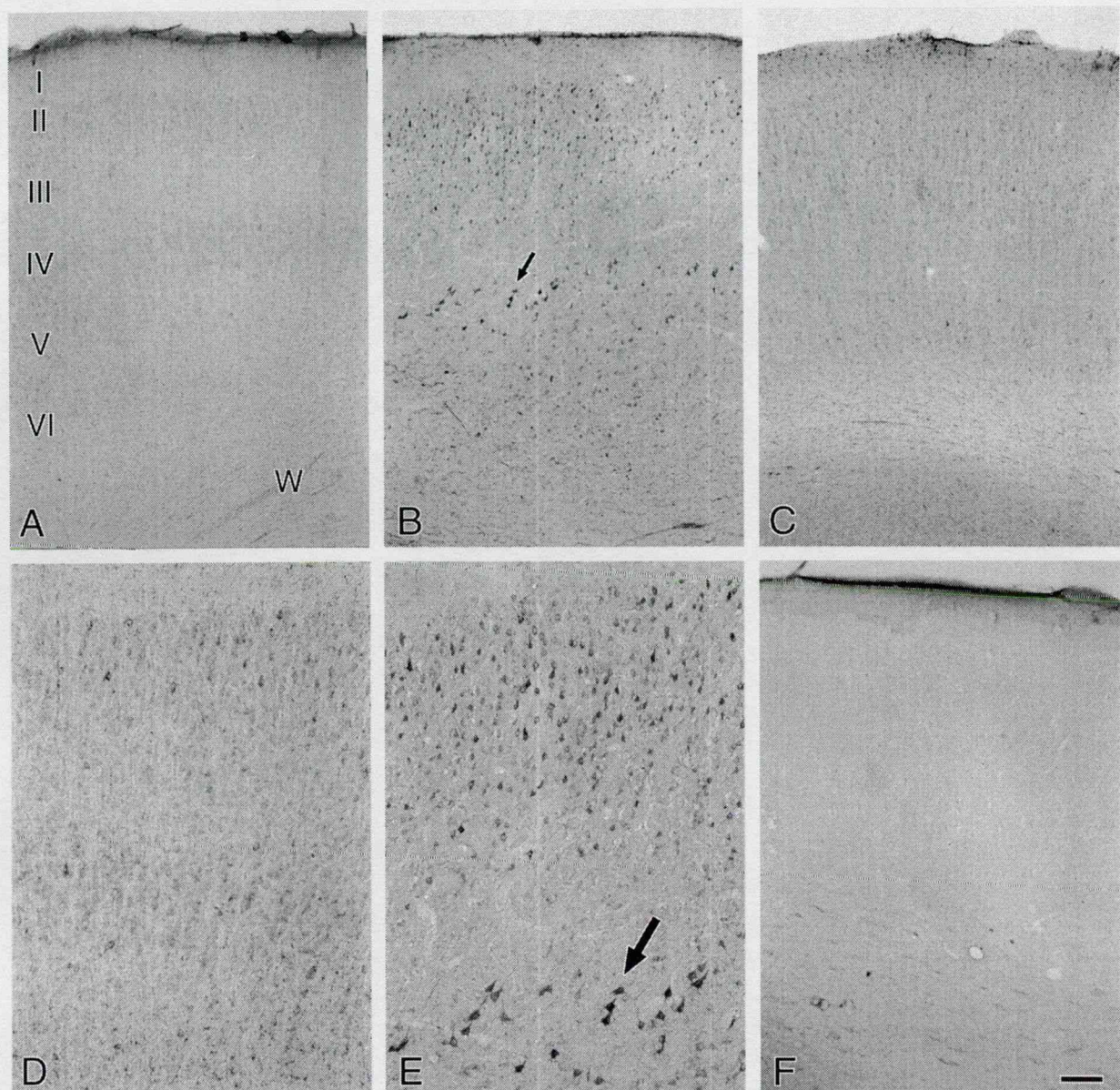


**Figure 2.**

Effect of anoxic stress on COX-2 immunoreactivity in 50  $\mu$ m sections from cerebral cortex. A) Parietal cortex from 8 hr sham time control piglet showing uniform COX-2 staining primarily in cortical layers II/III, V, and VI. Some staining of smaller cells can be observed in the white matter (W). Roman numerals indicate cortical layers. B) COX-2 immunoreactivity was increased 8 hrs after global cerebral ischemia in cortical layers II/III, V and VI. Arrow indicates characteristic neuron which can be seen at higher magnification in panel E. C) Asphyxia did not appear to alter the intensity or pattern of COX-2 staining in parietal cortex. D) Higher magnification of time control parietal cortex shown in panel A. E) Higher magnification of ischemia parietal cortex shown in panel B. F) COX-2 immunoreactivity following preadsorption of primary antibody with COX-2. Scale bar = 200  $\mu$ m in A, B, and C. 120  $\mu$ m in D, E, and F.

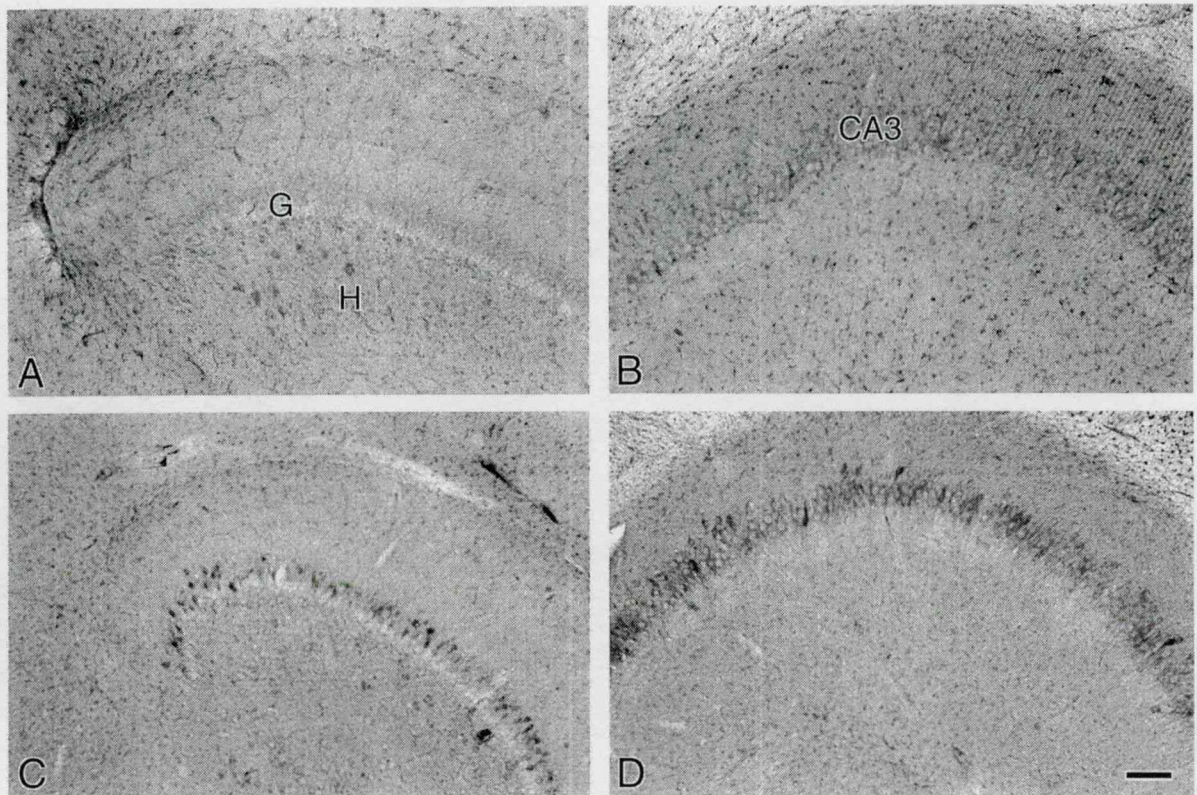


**Figure 3.**

Immunolocalization of COX-2 in 50  $\mu$ m sections from hippocampus after anoxic stress. A) Suprapyramidal blade of the dentate gyrus from a time control piglet. COX-2 immunoreactivity was consistently observed in a distinct patch of neurons in the polymorphic layer of this area. B) The CA3 pyramidal layer of time control piglets had modest to low levels of COX-2 immunoreactivity. C) At 8 hrs after global cerebral ischemia, COX-2 immunoreactivity was observed in the granule layer of the dentate gyrus. Concomitantly, there was a decrease in COX-2 staining of the polymorphic neurons in this region. D) An increase in COX-2 immunostaining of filed CA3 neurons occurred after global cerebral ischemia. Scale bar = 120  $\mu$ m.

the hippocampal fissure (Fig. 3A,B). The pattern of COX-2 staining in the time control animals was virtually identical to that in the untreated piglets (not shown).

### c. Cerebellum

Immunostaining for COX-2 was present at various intensities in the Purkinje cells and in the molecular and granular layers of the cerebellum (Fig. 4A). As in the parietal cortex and hippocampus, COX-2 IR-ity was detected in both neurons and glial cells. For example, a few cells were consistently observed in the granular layer and most likely represented neurons (Fig. 4B). Although the Purkinje cells themselves were never COX-2-positive, small cells adjacent to them were immunoreactive (IR) for COX-2 and GFAP. These small cells were probably Bergmann glia, as suggested by double labeling against GFAP and COX-2. The thin processes that displayed COX-2/GAfp IR-ity in the molecular layer appeared to be mostly the processes of the Bergmann glia, which are known to extend to the pial surface, but some could also be the processes of the granule cells (Fig. 4B).

## **Cellular localization of nNOS**

### a. Cortex

Unlike COX-2, the nNOS staining in the parietal cortex was quite sparse, but was observed in all cortical layers (Fig. 5C). Interestingly, there did not appear to be a particular subset or group of cells that were nNOS-positive. Virtually no IR-ity was detected in the white matter (Fig. 5C). The cell-specific staining of nNOS also differed from that observed for COX-2 (compare Fig. 5D and 5F). Very intense IR-ity was observed in the soma of large neuron-like cells. Moreover, the processes of these cells were IR for nNOS (Fig. 5F). As with COX-2, these cells are most probably neurons.

### b. Hippocampus

The hippocampus displayed a distinct staining pattern for nNOS (Fig. 6). Although scattered, intensely labeled cells were observed throughout the hippocampus, the nNOS IR-ity was primarily localized to the granule cell layer of the dentate gyrus and the mossy fiber layer (Fig. 6A). Higher magnification of the suprapyramidal blade of the dentate gyrus region revealed perinuclear nNOS IR-ity in the granule cell layer and occasional IR cells in the polymorphic layer (Fig. 6B). However, unlike the COX-2 staining, a distinct aggregate of nNOS-stained cells was never observed in the subgranular layer (compare Figs 7B and 6B). In addition to the somal staining of the granular cells, their axons, which comprise the mossy

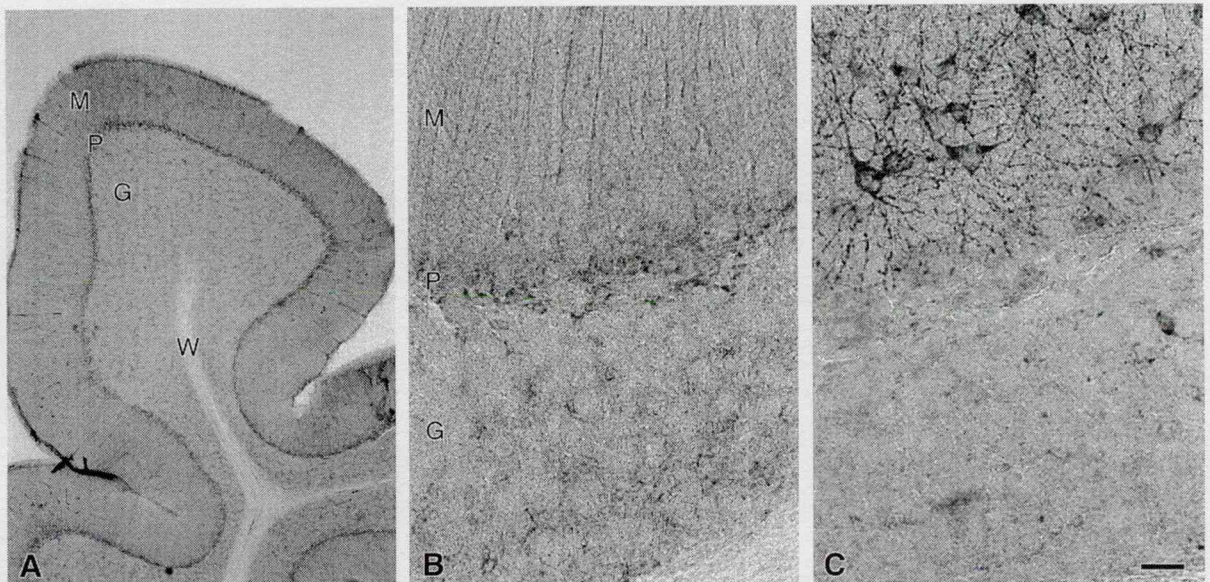


**Figure 4.**

Immunolocalization of COX-2 and nNOS in cerebellum. A) COX-2 immunoreactivity was observed in the molecular layer (M), Purkinje layer (P), and the granular layer (G). However, COX-2 staining was never detected in the white matter (W). B) The most prominent COX-2 immunoreactivity was localized to small cells in the Purkinje cell layer. These cells are most likely Bergmann glia. Note that the Purkinje cells themselves do not appear to be stained for COX-2. Processes of the Bergmann glia in the molecular layer and occasional cells in the granular layer were also COX-2 positive. C) The majority of nNOS immunoreactivity was localized to neuron-like cells, which may be basket cells, in the molecular layer. Like COX-2, the Purkinje cells lacked detectable nNOS immunoreactivity. Scalebar = 200 $\mu$ m in A; 25  $\mu$ m in B and C.

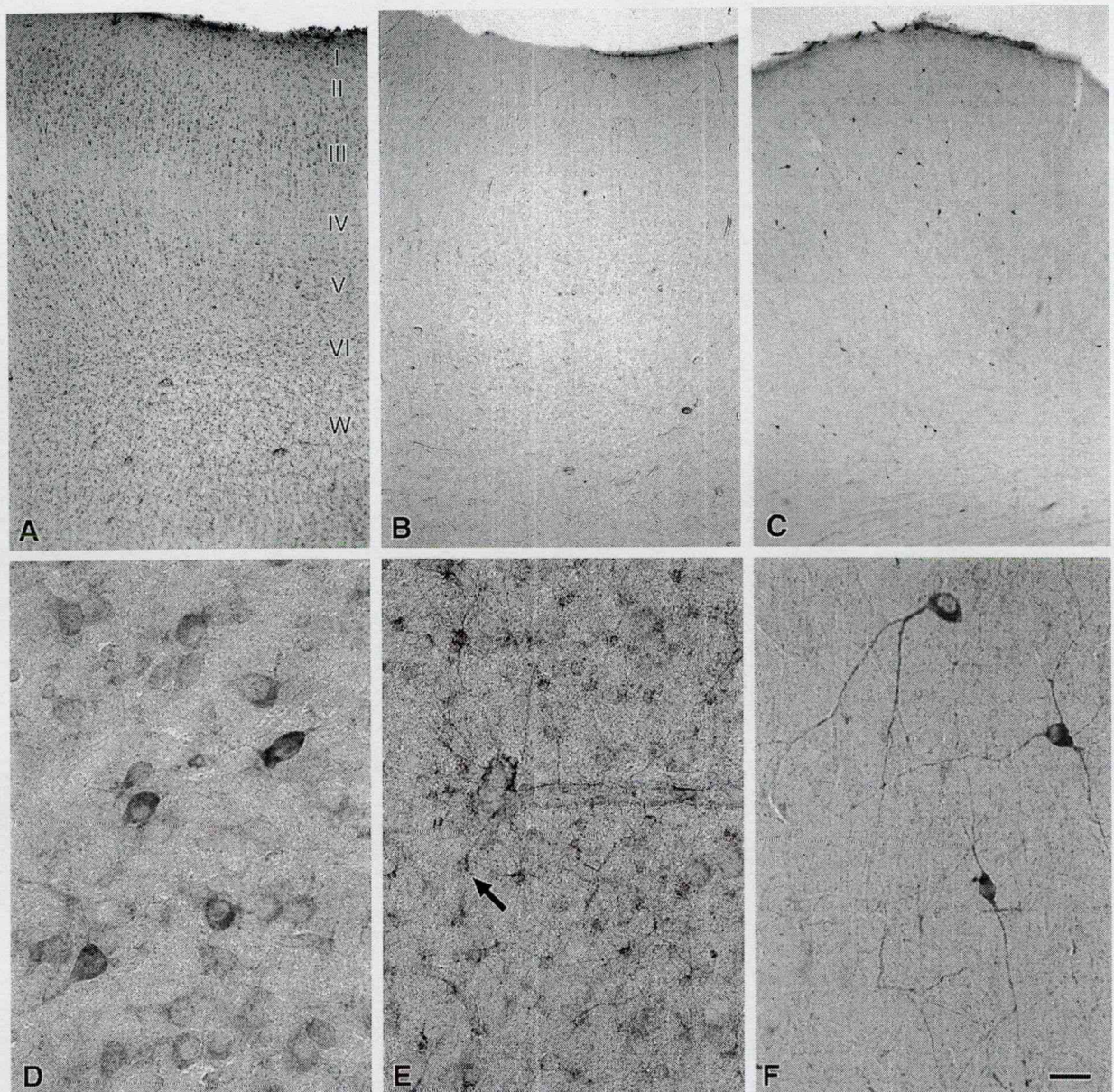


**Figure 5.**

Immunolocalization of COX-2 and nNOS in parietal cortex. A) Extensive cellular COX-2 immunoreactivity was evident in specially in cortical layers II/III, V, and VI, and white matter (W). Roman numerals indicate cortical layers. B) Omission of COX-2 antibody revealed only minimal background immunoreactivity. C) Immunostaining for nNOS was very sparse and localized primarily to neuronal cell types in cortical layers II-VI. Note absence of immunoreactivity in white matter. D) Representative photomicrograph of cortical layers II/III showing COX-2 immunoreactivity localized primarily to cell bodies at various degrees of intensity. E) COX-2 immunoreactivity in white matter revealed numerous small, multipolar cells projecting stained processes to adjacent blood vessels (arrow). F) Representative photomicrogram of cortical layers II/III showing nNOS staining in both cell body and processes of neuron-like cells. Scale bar = 200  $\mu$ m in A-B; 25  $\mu$ m in D-F

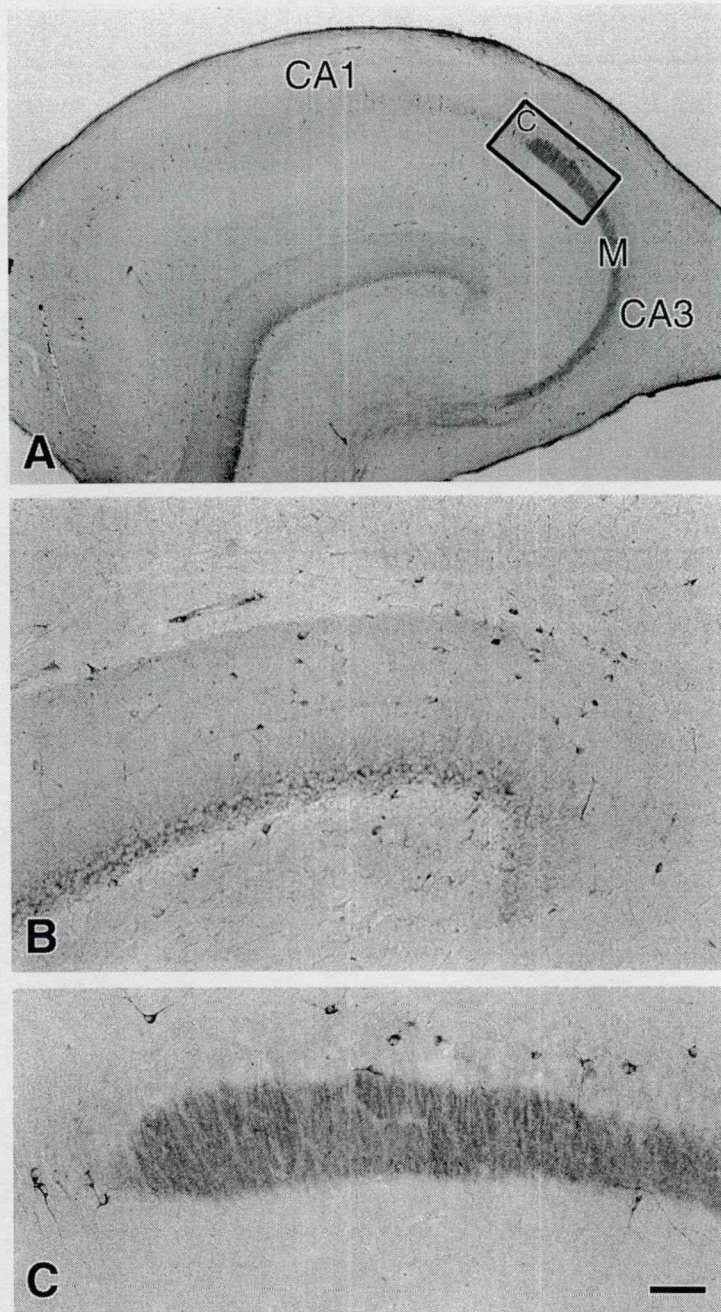


**Figure 6.**

Immunolocalization on nNOS in hippocampus. A) Representative cross-section of hippocampus showing pattern of nNOS immunoreactivity. Although occasional nNOS immunoreactive cells were observed throughout the hippocampus, the granular layer and mossy fiber layer (M) displayed the greatest staining. Very few cells were observed in the pyramidal cells in CA1 and CA3. B) Higher magnification of the apical region of the dentate gyrus. Neuronal NOS immunoreactivity appears to be localized to the cell bodies of the granular cells. C) Higher magnification of boxed area in panel A. Only occasional pyramidal and/or interneurons display nNOS immunoreactivity. However, the mossy fiber layer, which contains the axons of the granular cells, were consistently stained with nNOS. Scale bar=1840  $\mu$ m. in A, 120  $\mu$ m in B, and 368  $\mu$ m in C.

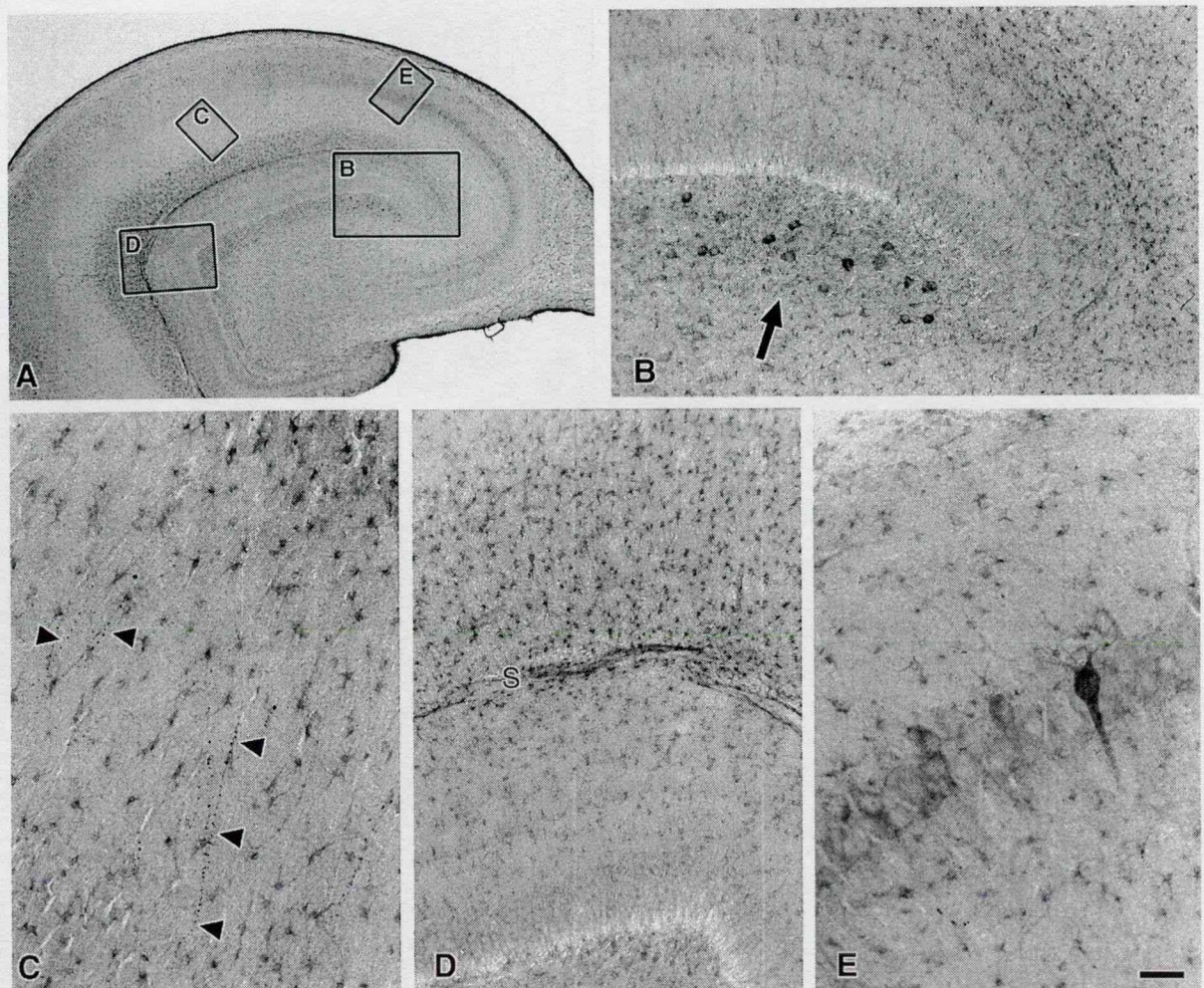


**Figure 7.**

Immunolocalization of COX-2 in hippocampus. A) Cross section of hippocampus showing anatomy of hippocampus and extensive COX-2 immunoreactivity. The boxed areas indicate the location of significant cell specific COX-2 reactivity in several areas, including (B) dentate gyrus, (C) stratum radiatum, (D) area adjacent to the hippocampal sulcus, and (E) CA3 pyramidal cells. These areas are shown at higher magnification in panels B-E. B) COX-2 immunoreactivity was consistently observed in the soma of a group of neuron-like cells in the subgranular region located at the inner tip of the dentate gyrus. The arrow denotes an aggregate of these cells. C) In the stratum radiatum, small, multipolar cells displayed immunoreactivity. Often processes were observed to contain areas of intense COX-2 staining (arrowheads). D) Numerous small COX-2 staining cells were located along the hippocampal sulcus (S). E) Pyramidal cells in CA3 displayed various intensities of COX-2 immunoreactivity. Scale bar = 1840  $\mu$ m in A, 20  $\mu$ m in B, 50  $\mu$ m in C,

fiber layer, were also nNOS-IR (Fig. 6C). Only occasional pyramidal cells and/or interneurons in this region were stained for nNOS. Interestingly, the nNOS-IR mossy fiber layer appeared adjacent to the CA3 pyramidal cells which are COX-2-positive (compare Figs 7E and 6C). The distinct pattern of nNOS IR-ity appears to complement the COX-2 IR-ity in the dentate gyrus and the CA3 pyramidal layer of the hippocampus.

#### a. Cerebellum

The pattern of nNOS staining in the cerebellum differed greatly from that of COX-2 (compare Fig. 4B and 4C). The only cells with detectable nNOS IR-ity were located in the molecular layer adjacent to the Purkinje cell layer (Fig. 4C). Intense nNOS IR-ity was localized to the cell body and the abundant processes of these cells. From morphologic considerations, the nNOS-stained cells in the molecular layer appear to be basket cells.

### Effect of anoxic stress on COX-2 patterns

#### a. Cerebral cortex

Global cerebral ischemia increased the intensity of COX-2 IR-ity in the parietal cortex (compare Fig. 2B and 2A). The increase in COX-2 IR-ity occurred primarily in the cortical layers which contained basal COX-2 staining (i.e. II/III, V and VI). At higher magnification, the perinuclear staining of the pyramidal neurons could be observed within cortical layers II/III and V (Fig. 2D (time control), and 2E (ischemia)). COX-2 IR-ity was also evident in the proximal portion of the apical processes of the intensely stained neurons (Fig. 2E). Unlike ischemia, whole-body asphyxia did not appear to alter the pattern or intensity of COX-2 IR-ity in the parietal cortex (Fig. 2C).

Sections of the visual cortex from a time control animal and from an animal 8 hours after the induction of global cerebral ischemia are shown in Fig. 8. Preadsorption of the antisera with purified COX-2 before incubation with sections resulted in a low background IR-ity and no identifiable neuronal structures (Fig. 8B).

The time control cortex (Fig. 8A) contained IR COX-2 neurons located primarily in cortical layers II and V. However, some COX-2 IR neurons were scattered throughout the gray matter of the visual cortex, in definite layers. The neuronal COX IR-ity was increased markedly, especially in cortical layers II/III and V, 8 hours after ischemia (Fig. 8B). Increases in both the staining intensity of the individual neurons and the number of COX-2 IR neurons were apparent. Subcellularly, COX IR-ity filled the cytoplasm and was concentrated in perinuclear

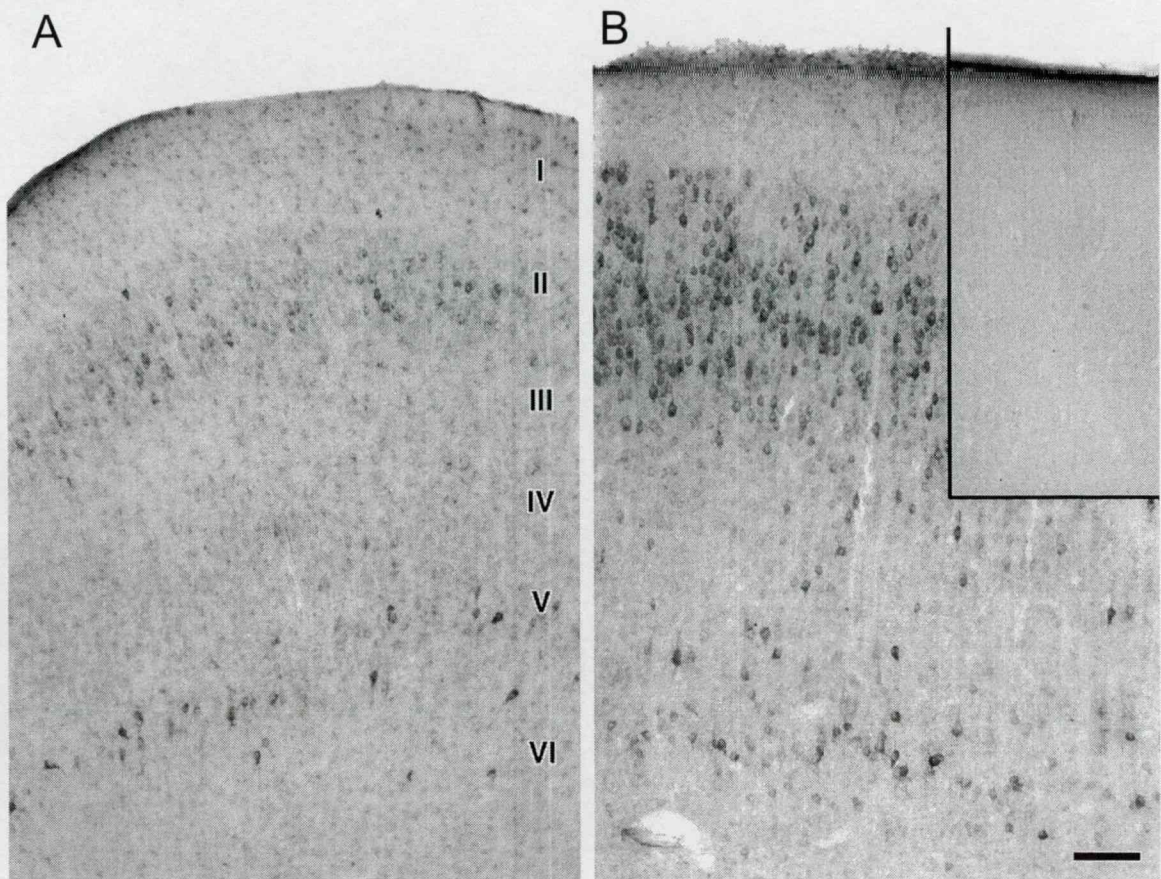


**Figure 8.**

Effects of ischemic stress on visual cortex COX-2 immunoreactivity. A) Modest COX-2 IR in scattered neurons localized to cortical layers II and V in a section from an 8 hour time control animal. Roman numerals indicate cortical layers. Insert: Only minimal background COX-2 IR was seen in section of visual cortex following preadsorption of COX-2 antisera with purified COX-2 antigen. B) Increased COX-2 IR was observed in a section 8 hr after cerebral ischemia. The most prominent changes in immunoreactivity were in layers II/III, but an increase in labeled neurons also was prominent in layers V. Scale bar: 100  $\mu$ m.

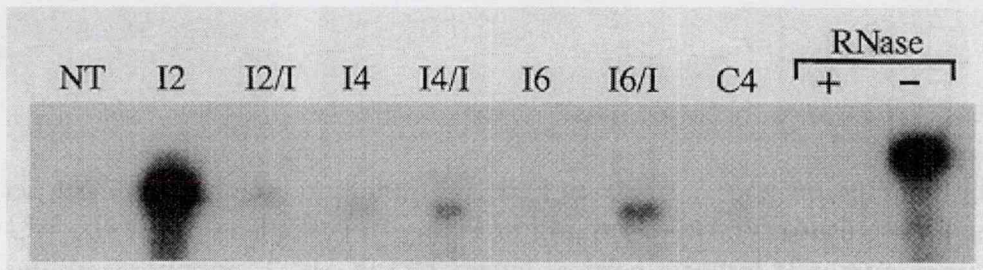


**Figure 9.**

Effects of indomethacin pretreatment (5mg/ kg, i.v.) on COX-2 mRNA in hippocampus following ischemia. Indomethacin pretreatment (I) attenuated the large increase in mRNA normally seen early after ischemia. Lane designation are the same as used in Figs. 13-15.

areas of the neuronal soma, extending into the apical dendrite in very heavily stained neurons (not shown).

### b. Hippocampus

Global cerebral ischemia altered the pattern of COX-2 IR-ity primarily in the polymorphic and granule layers of the dentate gyrus and in field CA3 of Ammon's horn. By 8 hours after ischemia, virtually no subgranular neurons in the polymorphic layer of the dentate were IR for COX-2 (Fig. 3C). Instead, intense COX-2 IR-ity was localized to cells within the granule layer of the dentate gyrus (Fig. 3C). Further, the intensity of COX-2 IR-ity in the pyramidal neurons in CA3 was greater and more consistent than in the time controls (Fig. 3B,D). While the COX-2 IR-ity was greatly increased in both the dentate granule and the CA3 pyramidal layers, no detectable changes were observed in the staining of the small stellate cells bordering the hippocampus. Unlike ischemia/reperfusion injury, no detectable changes in either the pattern or the intensity of COX-2 immunostaining were observed after whole-body asphyxia (not shown). Thus, global cerebral ischemia increased not only the intensity of the staining in the pyramidal cells of Ammon's horn, but also the COX-2 immunostaining in the granule cells of the dentate gyrus.

#### *Indomethacin treatment*

Systemic pretreatment with indomethacin prevented the increases in COX-2 mRNA at 2 hours after ischemia (Fig. 9). Indomethacin pretreatment also prevented the increases in COX-2 IR-ity at 8 hours after ischemia in the hippocampus (Fig. 10) and cerebral cortex (not shown).

#### *7-NI treatment*

Systemic pretreatment with 7-NI did not prevent the increases in mRNA for COX-2 (not shown) following ischemia. Further, 7-NI pretreatment had no substantial, consistent effect on the increases in COX-2 IR-ity at 8 hours after ischemia in the hippocampus (Fig. 11) and cerebral cortex (not shown).

### **COX-2 expression in the retina**

A section of retina stained with cresyl violet is shown in Fig. 12A for orientation. From the outside to inward, Seven layers are discernible. From the outside inwards, these are the photoreceptor (P) layer, the outer nuclear layer (ONL), the outer plexiform layer (OPL), the

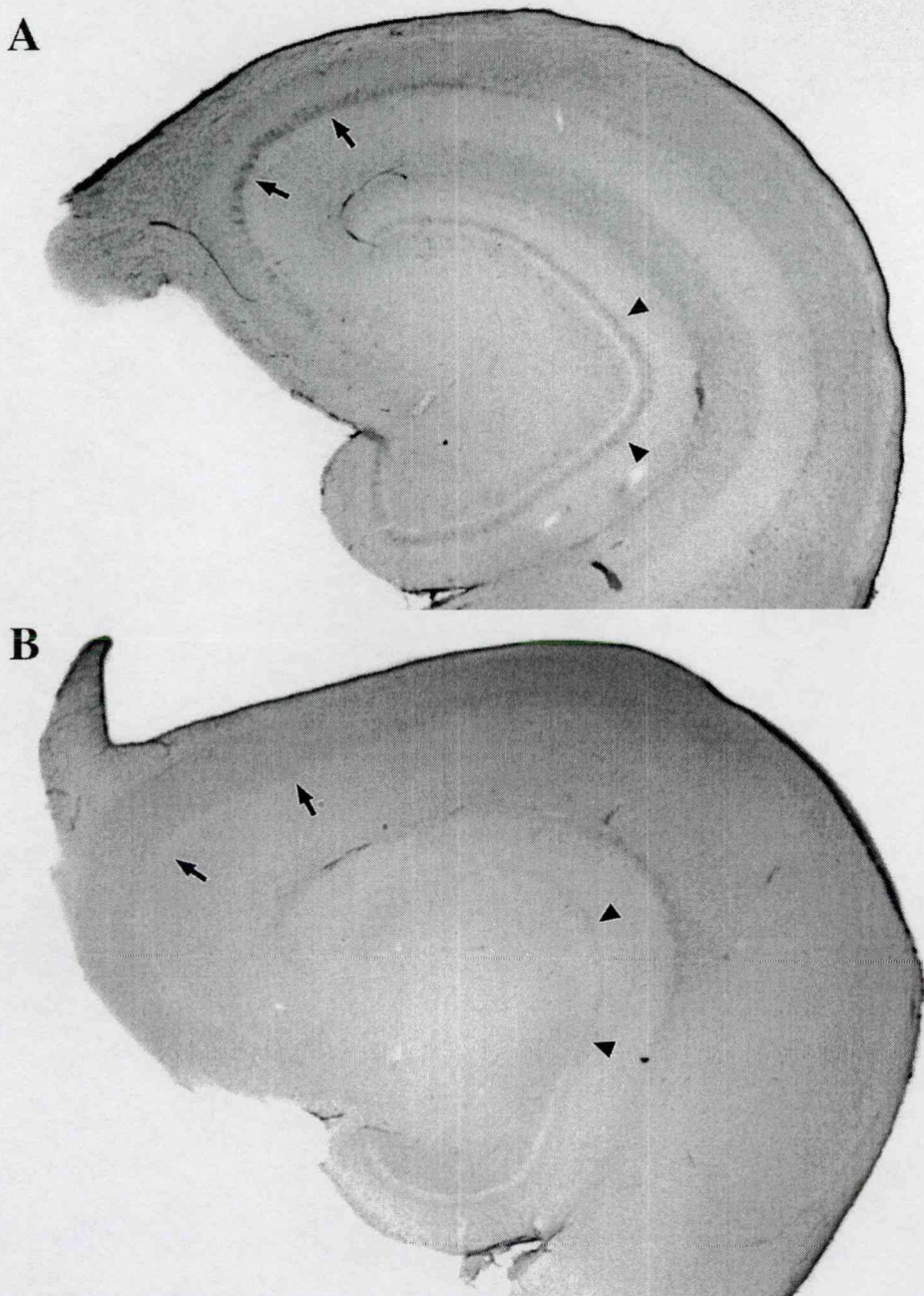


**Figure 10.**

Effects of indomethacin pretreatment (5mg/kg, iv) on immunolocalization for PGHS-2 8 hours after ischemia on 50  $\mu$ m sections from hippocampus. A: Ischemia increased PGHS-2 immunostaining in field CA3 neurons (arrows) and in the polymorphic layer of the dentate gyrus (points). B: Indomethacin pretreatment completely eliminated increased immunostaining for PGHS-2 in these areas. Original magnification is 3.91X for A and 3.125X for B.

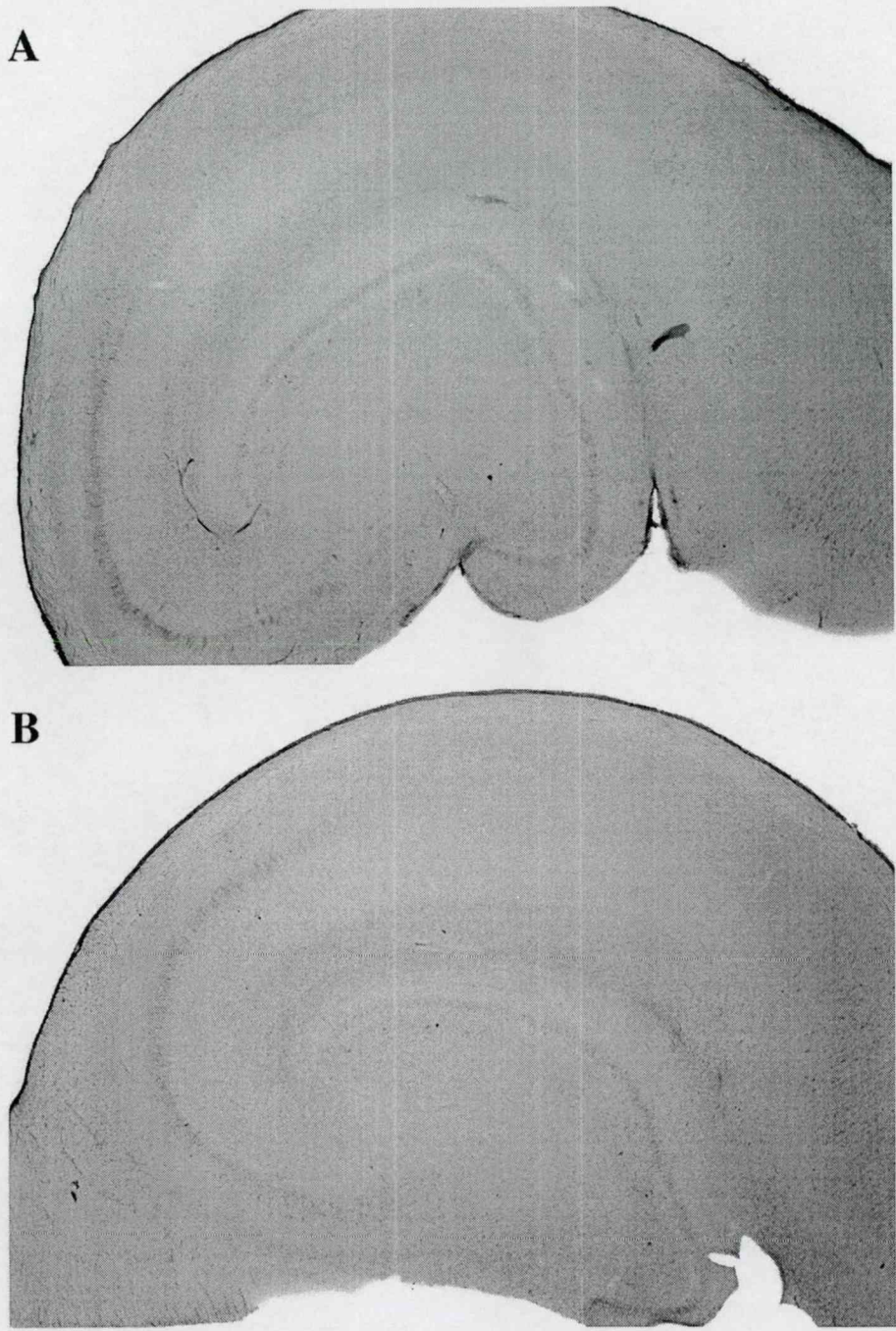


**Figure 11.**

Effects of 7-NI on immunolocalization for COX-2 8 hours after ischemia on 50  $\mu$ m sections from hippocampus. A) Ischemia alone. B) Ischemia following pretreatment with 7-NI (50mg/kg, ip given before ischemia, and also 4 hours after ischemia). There was no consistent effect of 7-NI treatment on increases in COX-2 immunoreactivity after ischemia. Original magnification is 3.125X for both A and B.

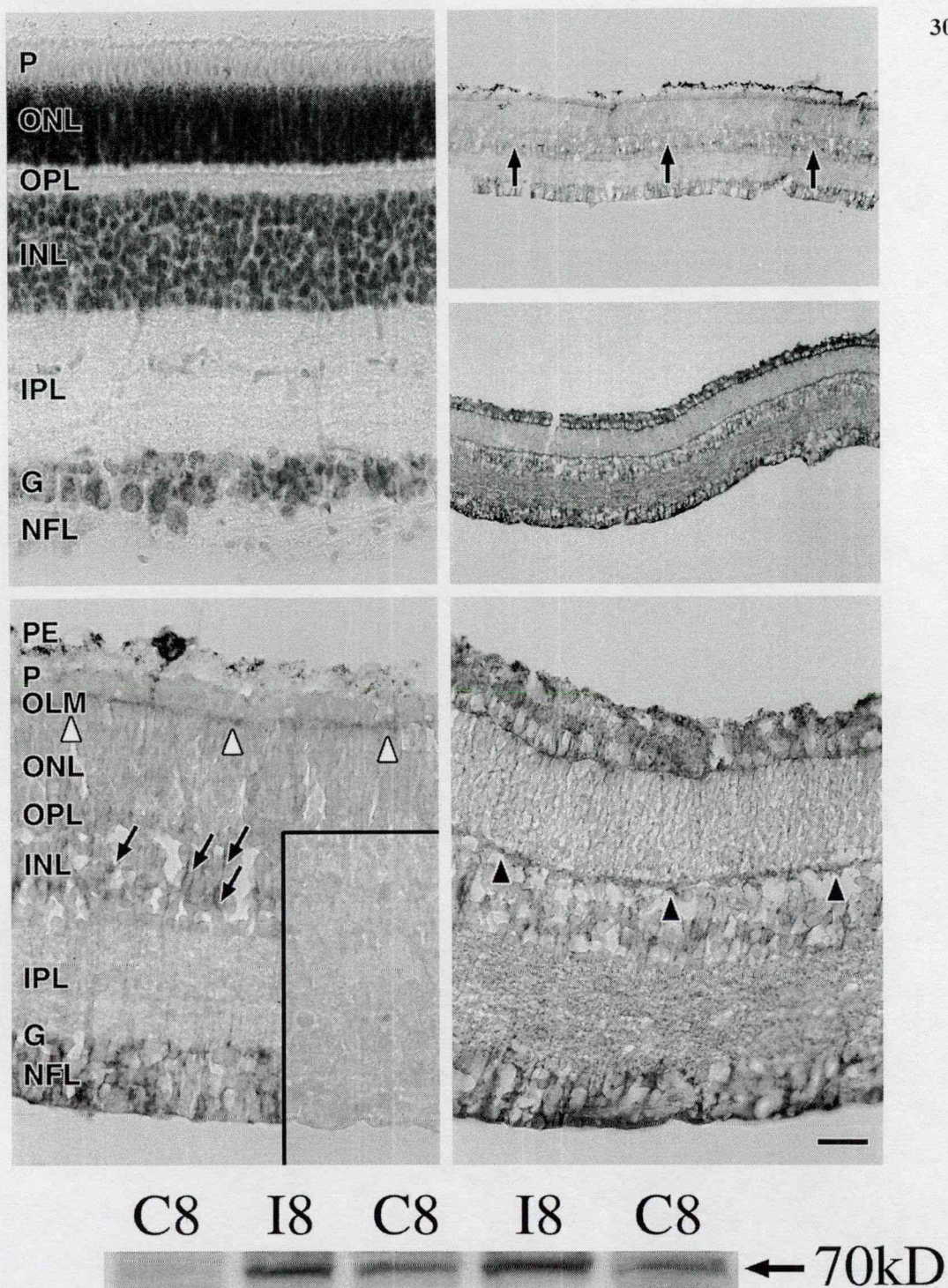


**Figure 12.**

Effects of ischemia on COX-2 immunoreactivity and immunoblotting of the piglet retina. Panel A depicts the laminar organization of the piglet retina after cresyl violet staining. Labels indicate photoreceptor (P), outer nuclear (ONL), outer plexiform (OPL); inner nuclear (INL), inner plexiform (IPL), ganglion cell (G), and nerve fiber (NFL) layers. Panels B-E indicate retinal sections stained for COX-2. B and D are low and high magnifications, respectively, of retina from untreated piglet. Arrows in B and D represent relatively heavy COX-2 immunostaining in cell bodies within the INL, which probably are Müller cells. White arrowheads in B indicate presence of COX-2 immunostaining in OLM. Moderate COX-2 IR is also associated with layers G and NFL. Insert in Fig. D demonstrates lack of immunostaining in a preimmune, control retina. C and E are low and high magnifications, respectively, of retina from a piglet 12 hours after ischemia. Obvious increases in COX-2 IR occur in P, OLM, OPL/INL interface, G, and NFL. The lack of increased immunostaining in the ONL after ischemia caused this layer to appear relatively unstained as compared to the other retinal layers (compare B and C). Scale bar 100  $\mu$ m for panels A, D and E, 66.6  $\mu$ m for insert in D, and 400  $\mu$ m for B and C. Panel F demonstrates increases in COX-2 protein levels 8 hours after ischemia in whole retina via immunoblotting. The immunoreactive band migrated at the appropriate molecular weight for COX-2 and previous studies have shown that pre-adsorption eliminated the band at this location.

inner nuclear layer (INL), the inner plexiform layer (IPL), the layer of ganglion cells (G) and the layer of optic nerve fibers (NFL). A clearly discernible outer limiting membrane (OLM) is also located between the ONL and P layer (Fig. 12D, arrowheads).

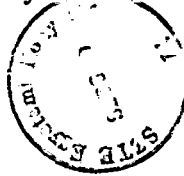
### Control conditions

Limited but detectable immunostaining for COX-2 was present in the control retinas and was layer-dependent. There were no major differences in immunostaining patterns between the untreated and the time control retinas (data not shown). Intact retinas immunostained for COX-2 are shown in Fig. 12B-E (a negative control is shown in the insert in Fig. 12D). The untreated retina exhibited COX-2 IR-ity localized to the OLM (Fig. 12D, arrowheads), with diffuse IR-ity throughout the ONL/OPL region. Moderately intense staining was also evident in scattered areas of the ganglion cell layer and in a line of cell bodies located in the midline of the INL. The location and morphology of these IR cells suggested that they were Müller cells. The INL staining appeared as a discontinuous chain (arrowheads) of IR-ity coursing through the INL (arrows) at the lower magnification (Fig. 12B,D). No COX-2 IR-ity above the background level was seen in other retinal layers. Preimmune technical control sections of the retina revealed no detectable COX-2 IR-ity (Fig. 12D, insert). The very dark areas at the surface of the photoreceptor layer (most noticeable in Fig. 12B,D) are fragments of pigment epithelium (PE) which were still present in some sections.

### Effects of ischemia

Ischemia induced a marked increase in COX-2 IR-ity in the neural retina (Figs. 12C, 12E). After an 8 (data not shown) or 12-hour period of recovery from 10 minutes of ischemia, the IR COX-2 level was elevated in all layers of the retina except the ONL/OPL, with the greatest increases seen throughout the photoreceptor layer, including the OLM. COX IR-ity was distributed in some areas along the full length of the photoreceptors into the outer segments. A discontinuous row of IR COX-2 elements also became apparent after ischemia in the vicinity of the OPL/INL interface, which that was not seen in the untreated or time control retinas. This is particularly evident in the low-magnification view in Fig. 12C. The absence of significant COX-2 IR-ity in the ONL after ischemia caused this layer to appear unstained as compared to the increased immunoreactivity of the other retinal layers.

The Müller cell COX-2 IR-ity (arrows in Fig. 12B,D) also appeared to be increasing, as evidenced by an increase in cytoplasmic IR-ity in cell soma located in the midline in the INL



and in the basal and apical membranes, but these increases were more subtle. Moderate to substantial COX IR-ity was present in the IPL, GL and NFL.

Immunoblotting using the whole retina supported the immunostaining results (Fig.12F). Thus, the COX-2 protein level in the whole retina was increased dramatically by 8 hours after ischemia.

#### *RNase protection assay*

Changes in COX-2 expression following anoxic stress

#### Regional variations in the brain

Global cerebral ischemia transiently increased the expression of COX-2 mRNA in the parietal cortex and hippocampus (Figs 13-15). In the cerebral cortex, the upregulation of COX-2 mRNA was variable; it occurred at 2-4 hours and returned to the control levels by 8 hours (Fig. 13, top; Fig. 14). For the cortex, we converted the densities of bands into pixels, using the NIH Image Analysis software (version 1.55). The densities of mRNA for cortex were  $886 \pm 234$  pixels (mean  $\pm$  standard error) for the time control animals ( $n=16$ ),  $3430 \pm 2136$  pixels for animals 2 hours after ischemia ( $n=7$ ),  $5257 \pm 1319$  pixels for animals 4 hours after ischemia ( $n=8$ ), and  $1385 \pm 33$  pixels for animals 8 hours after ischemia ( $n=2$ ) ( $P<0.05$ , time control versus 4-hour ischemia animals). For the hippocampus, increased COX-2 mRNA levels occurred consistently at 2 hour after ischemia (Fig. 13, middle; Fig. 15). Further, COX-2 mRNA remained only slightly increased over the control levels at 4 and 8 hours after the ischemia in hippocampus. Increases in mRNA for COX-2 occurred in other areas of the brain within 2-4 hours after ischemia, e.g. in the cerebellum (Fig. 13, bottom) and in the superior colliculus and thalamus (not shown). Use of the sense probe for COX-2 failed to produce bands on the gel (Fig. 14).

In contrast with ischemia, asphyxia did not appear to alter the COX-2 mRNA levels throughout the 8-hour reoxygenation period in the hippocampus (Fig. 15) or in the cerebral cortex or cerebellum (not shown). Thus, the increased COX-2 mRNA synthesis appeared to be sensitive to the mode of anoxic stress employed.

#### In the retina

COX-2 mRNA levels were not detectable in the non-treated or time control retina at 2 hours, but by 1 and 2 hours after ischemia the level had increased considerably (Fig. 6). At 4 hours

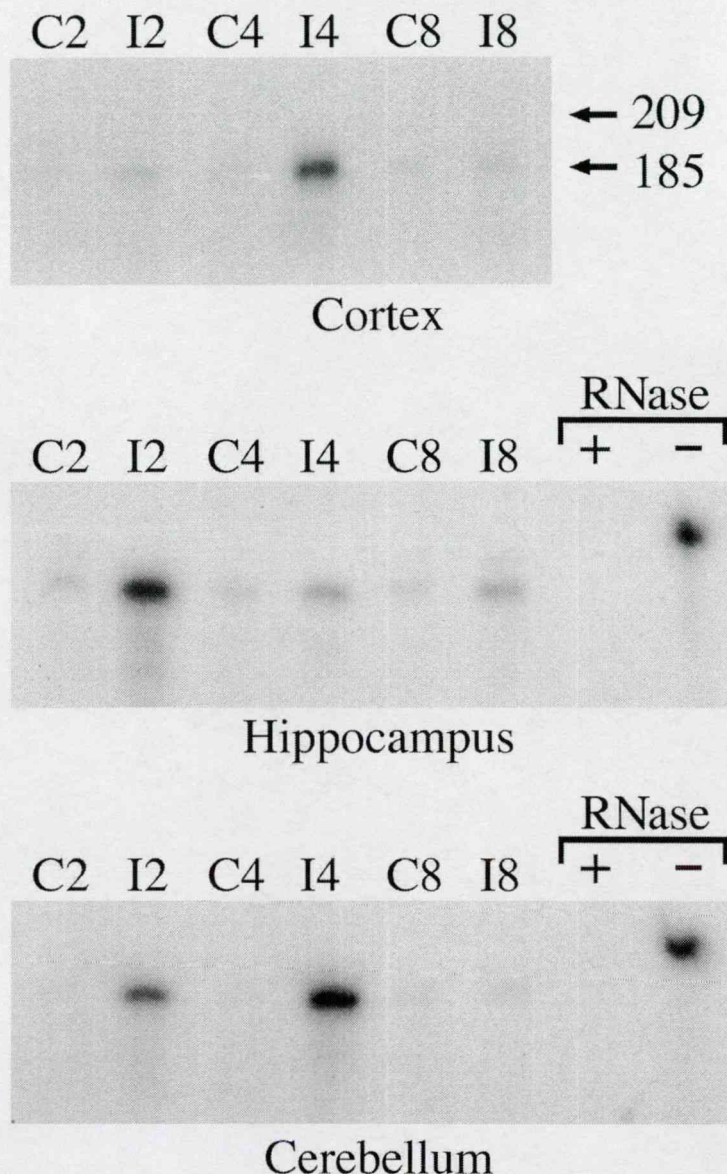


**Figure 13.**

Upregulation of PGHS-2 mRNA after global cerebral ischemia. RNase Protection Assay revealed increased expression of PGHS-2 mRNA at 2-4 hrs in cerebral cortex, hippocampus, and cerebellum. The 2, 4, and 8 hr time control lanes are indicated as C2, C4, and C8, respectively. Likewise, 2, 4, and 8 hrs after ischemia are indicated as I2, I4, and I8, respectively. Unprotected probe digested with RNase is shown in '+' lane, while the unhybridized, undigested probe is shown in the '-' lane. Lane labels for the hippocampus and cerebellum blots are identical to those of the cortex. Note that the unprotected band shown in the last lane of the hippocampus and cerebellum blots runs at 209 bp and the hybridized bands migrate at 185 bp.

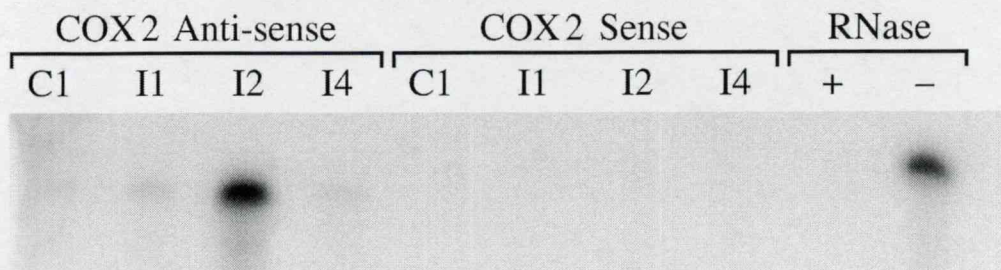


**Figure 14.**

Comparison of bands of protected fragments of COX-2 mRNA from hippocampus run with anti-sense and sense probes. RNA samples used with anti-sense and sense probes are aliquots from the same stock. The sense probe did not detect mRNA. Lanes as labeled in figure 13.

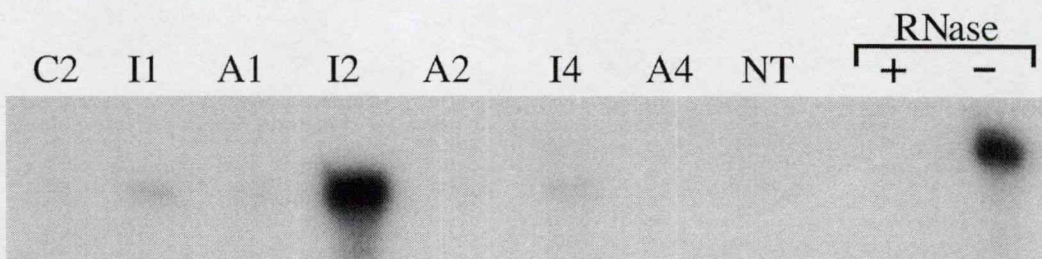


**Figure 15.**

Comparison of the effects of global cerebral ischemia and whole body asphyxia on PGHS-2 mRNA in hippocampus. A transient increase in PGHS-2 mRNA occurred after cerebral ischemia while no change was detected within 4 hrs after asphyxia. Note that there is also very little difference between the 2 hr time control band (C2) and the untreated band (NT). The ischemia lanes are indicated by 'I' and asphyxia lanes are indicated by 'A'. The numbers refer to the time after anoxic stress. The PGHS-2 probe lanes are as marked in figure 2.

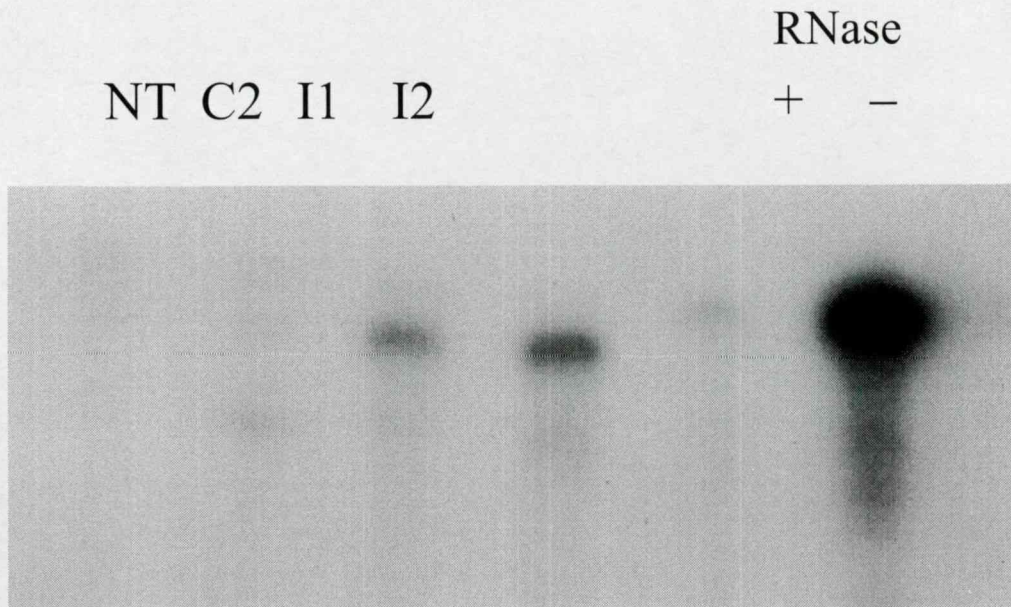


**Figure 16.**

**COX-2 mRNA expression in the piglet retina after ischemia.** Autoradiograph from RNase Protection Assay illustrates very low COX mRNA levels from a naive control (NT) and from a 2 hr time control animal (C2). Expression of COX-2 mRNA is increased 1 and 2 hrs after ischemia (I1 and I2). Unhybridized antisense probe digested with Rnase is shown in "+" lane, while unhybridized, undigested anti-sense probe is shown in "-" lane. The unhybridized probe band shown in the last lane runs at 209 bp and the hybridized, protected fragments migrate at 185 bp.

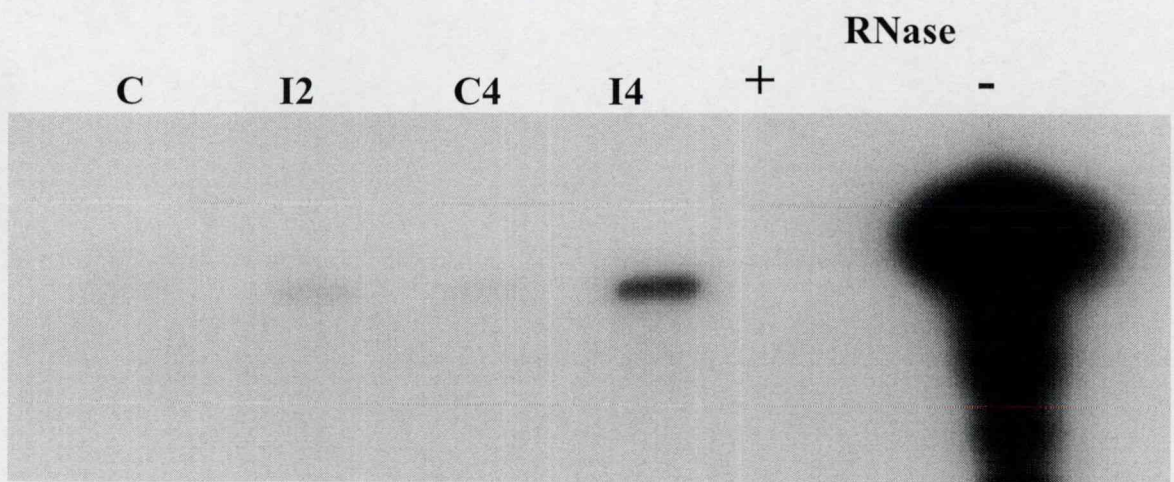


**Figure 17.**

**Upregulation of COX-2 mRNA in the visual cortex after ischemia.** RNase Protection Assay revealed increased expression of COX-2 mRNA in the occipital cortex in animals surviving 2 or 4 hrs after ischemia (I2 and I4). The 2 and 4 hr time-controls are indicated as C2 and C4. Unhybridized probe digested with RNase is shown in "+" lane, while the unhybridized, undigested probe is shown in the "-" lane.

after ischemia, the mRNA levels were not different from the 1-hour control values (data not shown).

COX-2 mRNA levels were barely detectable in the untreated or time control retina at 2 hours in the occipital cortex (Fig. 17), but the levels increased after ischemia and peaked by 4 hours. In technical control experiments, no bands were evident in those lanes where total RNA samples were hybridized with sense riboprobes transcribed from the cDNA template (data not shown).

### Discussion

Our studies have disclosed several new findings. First, COX-2 is the predominant COX isoform in the brain of the newborn pig, and COX-2 IR-ity is detectable in the retina and in the cerebral regions investigated. Second, transient ischemic stress leads to enhanced levels of COX-2 mRNA within 2-4 hours and of COX-2 protein within 8-12 hours. In contrast, there is no increase in the COX-1 mRNA and protein levels. Interestingly, the COX-2 mRNA and protein levels fail to increase after asphyxia. Third, indomethacin pretreatment attenuates the increases in COX-2 mRNA and protein levels after ischemia, whereas 7-NI pretreatment exerts little protective effect.

Only a few studies have examined the localization of COX in the brains of various species. In general, immunohistochemical studies indicate that COX isoforms are well represented in the brains of adult monkeys (Tsubokura et al., 1991), sheep (Breder et al., 1992) and rats (Yamagata et al., 1993; Breder et al., 1995; Kaufmann et al., 1996). For example, COX-1 displays extensive immunostaining in the cerebral cortex and hippocampus of adult sheep and monkeys (Tsubokura et al., 1991; Breder et al., 1992). Our studies confirm and extend previous findings by documenting the location and extent of COX-ity within the piglet brain. Thus, COX-1 IR cells are barely found in the newborn brain. In contrast, a great number of COX-2-IR neurons and glial cells are located in the cerebral cortex, hippocampus, cerebellum and retina. Similarly as in piglets, COX-2 appears to be particularly prominent in the neonatal rat. Further, the COX-2 protein level is predominant over that of COX-1 in the cerebral vasculature of the piglet (Peri et al., 1995; Busija et al., 1996). Accordingly, mRNA for COX-2 is more abundant than COX-1 mRNA in the cerebral blood vessels (Peri et al., 1995). Finally, PG production in piglet cerebral tissues and vessels is largely reduced by a selective COX-2 inhibitor (Peri et al., 1995). The reason for the predominance of COX-2 in neurons

and glial cells in the perinatal period is unclear, but it has been suggested to be due to augmented synaptic activity during development (Yamagata et al., 1993; Adams et al., 1996; Kaufmann et al., 1996).

The immunohistochemical characteristics of COX-2 observed in the present experiments are consistent with results from previous *in vitro* (26) and *in vivo* studies (14). For example, COX-2 is present constitutively to varying extents in the neurons and glial cells of the developing central nervous system. In addition, COX-2 is concentrated in perinuclear areas and in the dendrites of the neurons and the terminal processes of the astroglia. The changes in COX-2 IR are specific and do not involve all cell types, and the responses in similar cell populations are variable. Finally, the increases in the COX-2 mRNA and protein levels are relatively rapid, occurring within a few hours.

The COX-2 IR pattern of the control retina was such that most immunopositive staining appeared in four regions, three of which are known to be associated with the Müller cell: 1) in a diffuse line at the level of the OLM, 2) in cell soma located in the middle of the INL, 3) in pockets of IR-ity between the ganglion cell nuclei, and 4) in scattered IR-ity throughout the ONL/OPL. The OLM marks the apical pole of the Müller cell, a bipolar cell that spans the entire thickness of the retina from the basal membrane to the photoreceptor layer. The nuclei of Müller cells are located within the INL, where they form a distinct median sublayer. Thus, COX-2 IR was seen in areas corresponding to the Müller cell soma and at the termination of both outer and inner processes. The diffuse IR-ity seen in the OPL/ONL region could be localized to only two cell types, photoreceptor cell bodies which are located in the ONL, or the Müller cell, which at this level forms velate sheaths around the photoreceptor cell nuclei. Although double immunostaining for GFAP/COX-2 was not carried out, on the basis of location and morphological features it is likely that these IR cells are Müller cell somata. The IR-ity seen at the OLM border and in the ganglionic layer is probably due to COX-2 in the Müller cell processes. Little COX-2 IR was apparent in the other neuronal cell types of the retina (the horizontal cell, the amacrine cell and the retinal ganglion cell), at least in the perinuclear areas.

As the physiological evidence suggests an important functional relationship between the COX and NOS systems in the brain, we investigated the anatomical relationships which may underlie such interplay.

Analysis of our immunohistochemical data showed that the nNOS patterns are distinct from those of COX-2 in all the brain regions investigated. The most obvious difference is that only a low percentage of the neurons exhibited nNOS IR-ity. This finding is similar to that reported in the cerebral cortex, hippocampus and cerebellum of postnatal 7-day-old rats. In the cerebral cortex, the nNOS immunostaining was relative sparse, but evenly distributed, whereas the COX-2 IR-ity was extensive and particularly heavy in several layers. In the hippocampus, populations of cells immunopositive for nNOS or COX-2 were quite distinct, although overlap occurred in several areas, such as the CA1/CA3. Finally, the cerebellum nNOS and COX-2 were located in distinct cell populations. The anatomical location of nNOS containing cells is consistent with the possibility of an NO-modulating COX function and *vice versa*. Although there is apparently little overlap between the two cell types, the nNOS neurons are located close enough to affect COX-2-containing cells in the cortex, hippocampus or cerebellum. Although considered a relative unstable compound, NO is able to diffuse for considerable distances in the brain and can affect prostanoid production (Salvemini et al., 1993; Stadler et al., 1993; Curtis et al., 1996; Busija, 1997; Busija and Thore, 1997). Once released, NO could combine with the COX-dependent superoxide anion to form peroxynitrite (Beckman et al., 1990; Beckman, 1991), which could damage adjacent cells.

Our results confirm and extend previous findings by our own laboratories and other, indicating that COX-2 protein synthesis is very sensitive to ischemic stress in the piglet central nervous system. Further, increased levels of COX-2 in the retina and in various regions of the brain will probably affect the function, maturation and susceptibility to stress in the nervous system, including the visual system of the developing animal. These results also demonstrate that the COX-2 levels are differentially affected by the type of anoxic stress, and that increases in COX-2 after ischemia are dependent on indomethacin- but not 7-NI-sensitive mechanisms.

The attenuation of ischemia-induced increases in the COX-2 mRNA and protein levels by indomethacin suggests that products of the AA metabolism lead to the upregulation of COX-2. The COX-dependent production of the superoxide anion or of prostanoids during the reperfusion period might activate nuclear factor (NF)-kappaB or other transcription factors and lead to enhanced COX-2 synthesis (Long and Pekala, 1996; Schmedtje et al., 1997). For example, indomethacin has also been reported to suppress the PGE<sub>2</sub>-induced transcription of corticotropin-releasing hormone (Markrigrannakis et al., 1996). In previous studies,

indomethacin pretreatment before ischemia has been shown to attenuate neuronal damage and to prevent increases in inducible for of heat shock protein 70 (iHSP70) and endothelial NOS (Beasley et al., 1998a, b). Thus, indomethacin may have a general effect in protecting the brain following ischemic stress and thereby inhibiting increases in stress-induced proteins. Alternatively, by preventing the production of oxygen radicals during the reperfusion period (Pourcyrous et al., 1993), indomethacin pretreatment may prevent the activation of NF- $\kappa$ B by reactive oxygen species (Sen and Packer, 1996). Since NO can have effects on PG synthesis or on the expression of COX *in vitro* (Salvemini et al., 1993; Busija and Thore, 1997; Habib et al., 1997), it was surprising that 7-NI had minimal effects on the increases in COX-2 IR-ity after ischemia. However, COX-2-immunopositive neurons may not be exposed to sufficiently high levels of brain-derived NO, since there is little overlap between nNOS and COX-2 IR-ity in the cerebral cortex and hippocampus in piglets. Alternatively, NO may be only one of many competing influences on COX-2 expression during ischemia/reperfusion.

The finding that the COX-2 mRNA and protein levels in the brain increase after ischemia, but not after asphyxia, was unexpected because the two stimuli are equally potent in producing superoxide anion in piglets (Pourcyrous et al., 1993). Additionally, it has been found that iHSP 70 increases to a similar extent in the brain after either asphyxia or ischemia. One possible reason for the difference in COX-2 responses between ischemia and asphyxia is that in the latter situation the systemic levels of CO<sub>2</sub> increase dramatically. Vannucci et al. (1995) reported that exposure to inhaled CO<sub>2</sub> is able to reduce brain damage in neonatal pups following hypoxia/ischemia. In contrast, hypercapnia has been shown to enhance damage during ischemia in adult rats (Katsura et al., 1994; Morimoto et al., 1993). Acidosis can suppress the activation of some (Frick et al., 1997), but not all (Yamaji et al., 1994) intermediate early genes. Since COX-2 induction in response to hypoxia in the endothelial cells is dependent upon the activation of NF- $\kappa$ B (Schmedtje et al., 1997), we speculate that acidosis or some other attribute of asphyxia leads to the suppression of this transcription factor.

Ischemia had dramatic, but variable effects on retinal staining. For example, the neurons and Müller cells exhibited enhanced COX-2 IR-ty, while the perinuclear areas of the photoreceptor cells showed little IR-ity. In contrast, the changes in the COX-2 distribution in the retinal neuronal elements after ischemia were more dramatic. After ischemia, a discontinuous line of COX-2 IR-ity was apparent at the OPL/INL interface. The dendritic

fields of bipolar neurons and horizontal cells are known to occupy this region, and the linear pattern of IR-ity might be due to increased COX-2 levels in the dendritic fields of either or both cell types. The modest increases in IR-ity seen in the other synaptic regions of the retina, the IPL, could also be attributed to the dendritic field of other retinal neurons, the amacrine cells, whose somata are located in the ONL or cell bodies of the ganglion cells. Alternatively, Müller cells are known to extend horizontal branches into this synaptic region.

There are two consequences of increased COX-2 levels following ischemia in piglets. First, as shown previously (Leffler et al., 1990), the prostanoïd production by the cerebral arteries and tissues, is increased following ischemic stress. Thus, prostanoïd-mediated effects on the cerebral circulation and/or brain function might be enhanced after ischemic stress. Secondly, increased COX-2 levels would lead to enhanced superoxide anion production during subsequent neurological sequelae. For example, seizure activity, the cessation of breathing and subarachnoid hemorrhage often occur following resuscitation after hypoxic/ischemic insults in babies (Vannucci et al., 1995; Volpe, 1994). The enhanced production of the superoxide anion under these conditions (Amstead et al., 1989; Mirro et al., 1989; Yamagata et al., 1993; Busija and Meng, 1993; Bari et al., 1996a) might result in further vascular and neuronal damage.

We have assessed the specificity of the COX-2 antibody and other reagents employed in immunostaining by using several procedures. First, we have demonstrated similar immunostaining for this and another COX-2 antibody from a different source, and use of either of these antibodies resulted a different staining pattern from that obtained when COX-1 antibodies were used (Thore et al., 1998; Domoki et al., 1999). Secondly, COX-2 immunostaining was eliminated following pre-adsorption with purified COX-2. Thirdly, the use of pre-immune serum or elimination of the COX-2 antibody led to minimal staining. And fourthly, Western blotting on the cerebral blood vessels (Domoki et al., 1999) confirmed the results from COX-2 immunostaining experiments. In the current study, we have shown that Western blotting and immunohistochemistry support the conclusion that ischemic stress increases the COX-2 protein levels in the retina.

Although it has been known for decades that COX inhibitors decrease cerebral ischemic injury, it has been assumed that the PG-s exacerbate the damage via their effects on inflammation or blood flow. Treatment with a COX-2-selective inhibitor has recently been shown to decrease the damage after temporary focal ischemia (Nogawa et al., 1997). Since

secondary hypoperfusion and inflammation are characteristic of this model, the observed neuroprotection could be caused by these mechanisms. However, the recent use of global ischemia models has yielded accumulating evidence that neuronal death in connection with COX-2 expression is a result of events that occur within the neuron. There are several pharmacological approaches which involve the inhibition of COX or the elimination of specific COX metabolites, supporting this view. A major investigation of the mechanism of inhibited N-methyl-D-aspartate-induced vasodilation in the brain provided evidence that COX-derived substances transiently disrupt the neuronal activity following anoxic stress. The inhibition of COX activity results in preserved NMDA-induced vascular responses. COX is a relatively unstable protein located intracellularly and it is eventually degraded during the metabolism of AA. Protein synthesis is therefore required for the continued production of prostanoids. On the other hand, COX is a primary source of the superoxide anion. Hence, as expected, the inhibition of protein synthesis also prevented ischemia-induced suppression of neuronal-vascular coupling in the cerebral cortex.

Recent studies indicate that the AA acid metabolism plays a definite role in the mechanism of perinatal hypoxic brain injury. Studies of postischemic hemodynamic changes in the cerebral circulation revealed that the inhibition of prostanoid synthesis preserves the major vasodilator mechanisms (Busija, 1997). A number of data indicate that the impaired vasorelaxation is associated with the production and action of free radicals during the reperfusion period. The superoxide anion is produced in the cortex during asphyxia and reventilation in piglets (Pourcyroux et al., 1993). Although there are several sources for superoxide and other free radicals after anoxic stress, all of them require O<sub>2</sub>. An O<sub>2</sub> load after asphyxia could enhance free radical production via either the mitochondrial or the arachidonate cascade. It seems that the COX pathway is the main source of superoxide in the brain of asphyxiated piglets (Pourcyroux et al., 1993) and also in the cerebral endothelial cells (Parfenova et al., 1997). The site of superoxide production is in the COX pathway when PGG<sub>2</sub> is converted to PGH<sub>2</sub> (Shimizu and Wolfe, 1990). Not only does the arachidonate cascade produce oxygen free radicals, but these can activate the cascade. Thus, superoxide production by this mechanism may result in a vicious cycle of accelerating radical production, which can lead to oxidant injury to the cells and tissues under pathological conditions (Shimizu and Wolfe, 1990, Pourcyroux et al., 1993).

Hypoxic/ischemic injury is a relatively common occurrence in the perinatal period, and is associated with immediate and sustained damage to the brain and the visual system. Our findings provide a basis for suggesting that the augmented COX-2 levels observed following ischemic stress may participate in the progression of these neuronal and retinal pathological processes. Nonetheless, more work is needed to establish a causative relationship between the increased COX-2 levels and the cellular vulnerability in the developing brain and visual system.

In conclusion, COX-2 is normally present in the retina and the various regions of the brain of the newborn pig, although the distribution of this enzyme is limited. However, global cerebral ischemia results in increased levels of COX-2 mRNA and protein within 2-8 hours. The enhanced levels of COX-2 could be a major source of free radicals, and PG-s and Tx-s in the injured brain, and could lead to disruption of the cellular and vascular functions and promote injury in the retina and the brain.

## **Acknowledgments**

A major part of this work was carried out during my two years leave in the United States, in the Departments of Physiology & Pharmacology and Ophthalmology, Wake Forest University, Bowman Gray School of Medicine, Winston-Salem, North Carolina.

I respectfully thank Professor David W. Busija for providing me with the opportunity to work at his laboratory. His kindness, patience and perfection enabled me to get familiar with an exciting area of the basic neuroscience. His quality work and devotion made a deep impression on me.

I wish to express my sincere gratitude to Professor Lajos Kolozsvári for his helpfulness and support that made my leave possible. In addition, I had the privilege of improving my skills in ophthalmology continuously under his chairmanship and he encouraged me to prepare this dissertation.

I am very thankful my coworkers, friends and colleagues Drs. Andrew Sweatt, Ferenc Domoki, Tracy Beasley, Clara Thore and Nishadi Thrikawala. Through each of them I learned a lot about science.

I thank my colleagues at the Department of Ophthalmology for their help during my clinical work.

I thank my husband, Ferenc Bari for his love and support.

## References

Abran, D., D. R. Varma, and S. Chemtob. Increased thromboxane-mediated contractions of retinal vessels of newborn pigs to peroxides. *Am. J. Physiol.* 268:H628-32, 1995.

Abran, D., D. R. Varma, D. Y. Li, and S. Chemtob. Reduced responses of retinal vessels of the newborn pig to prostaglandins but not to thromboxane. *Can. J. Physiol. Pharmacol.* 72:168-73, 1994.

Adams, J., Y. Collaço-Moraes, and J. de Belleroche. Cyclooxygenase-2 induction in cerebral cortex: An intracellular response to synaptic excitation. *J. Neurochem.* 66:6-13, 1996.

al-Zadjali, K. H., M. P. Imler, and S. E. Ohia. Inhibitory effect of prostaglandins on dopamine release from the retina. *Gen. Pharmacol.* 25:289-96, 1994.

Armstead, W. M., R. Mirro, C. W. Leffler, and D. W. Busija. Cerebral superoxide anion generation during seizure in newborn pigs. *Cereb. Blood Flow Metab.* 9:175-9, 1989.

Armstead, W. M., R. Mirro, D. W. Busija, and C. W. Leffler. Postischemic generation of superoxide anion by newborn pig brain. *Am. J. Physiol.* 255:H401-3, 1988.

Bari, F., R. A. Errico, T. M. Louis, and D. W. Busija. Differential effects of short-term hypoxia and hypercapnia on N-methyl-D-aspartate-induced cerebral vasodilatation in piglets. *Stroke.* 27:1634-9, 1996.a

Bari, F., R. A. Errico, T. M. Louis, and D. W. Busija. Interaction between ATP-sensitive K<sup>+</sup> channels and nitric oxide on pial arterioles in piglets. *J. Cereb. Blood Flow Metabol.* 16:1158-64, 1996.b

Bari, F., T. M. Louis, W. Meng, and D. W. Busija. Global ischemia impairs ATP-sensitive K<sup>+</sup> channel function in cerebral arterioles in piglets. *Stroke.* 27:1874-80, 1996.c

Bazan, N. G. Metabolism of arachidonic acid in the retina and retinal pigment epithelium: biological effects of oxygenated metabolites of arachidonic acid. In: Bito L. Z. and Stiernschantz J. (eds) *The ocular effects of prostaglandins and other eicosanoids*. Alan R. Liss. Inc. New York, pp. 15-37, 1989.

Bazan, N. G., and G. Allan. Signal transduction and gene expression in the eye: a contemporary view of the pro-inflammatory, anti-inflammatory and modulatory roles of prostaglandins and other bioactive lipids. *Surv. Ophthalmol.* 41. Suppl. 2:S23-34, 1997.

Beasley, T. C., F. Bari, C. Thore, N. Thrikawala, T. M. Louis, and D. W. Busija. Cerebral ischemia/reperfusion increases endothelial nitric oxide synthase levels by an indomethacin-sensitive mechanism. *J. Cereb. Blood Flow Metab.* 18:88-96, 1998.a

Beasley, T. C., F. Bari, C. Thore, N. Thrikawala, T. M. Louis, and D. W. Busija. Indomethacin attenuates early induction of cellular injury and iHSP 70 after cerebral ischemia/reperfusion in piglets. *Dev. Brain Res.* 105:125-35, 1998.b

Beckman, J. S. The double-edged role of nitric oxide in brain function and superoxide-mediated injury. *J. Dev. Physiol.* 1:53-9, 1991.

Beckman, J. S., T. W. Beckman, J. Chen, P. A. Marshall, and B. A. Freeman. Apparent hydroxyl radical production by peroxynitrite: implications for endothelial injury from nitric oxide and superoxide. *Proc. Natl. Acad. Sci. USA.* 87:1620-24, 1990.

Berger, R., and Y. Garnier. Pathophysiology of perinatal brain damage. *Brain Res. Rev.* 30:107-34, 1999.

Berger, R., and Y. Garnier. Perinatal brain injury. *J. Perinat. Med.* 28:261-85, 2000.

Birkle, D. L., and N. G. Bazan. Light exposure stimulates arachidonic acid metabolism in intact rat retina and isolated rod outer segments. *Neurochem. Res.* 14:5-90, 1989.

Breder, C. D. Cyclooxygenase systems in the mammalian brain. *Ann. N. Y. Acad. Sci.* 813:296-301, 1997.

Breder, C. D., D. De Witt, and R. P. Kraig. Characterization of inducible cyclooxygenase in rat brain. *J. Comp. Neurol.* 355:296-315, 1995.

Breder, C. D., W. L. Smith, A. Raz, J. Masferrer, K. Seibert, P. Needleman, and C. B. Saper. Distribution and characterization of cyclooxygenase immunoreactivity in the ovine brain. *J. Comp Neurol.* 322:409-38, 1992.

Buckley, N.M. Maturation of circulatory system in three mammalian models of human development. *Comp. Biochem. Physiol. A* 83:1-7, 1986.

Busija, D. W., C. Thore, T. Beasley, and F. Bari. Induction of cyclooxygenase-2 following anoxic stress in piglet cerebral arteries. *Microcirculation.* 3:379-86, 1996.

Busija, D. W. Eicosanoids and cerebrovascular control. In: Welch KMA, Caplan LR, Reis DJ, Siesjö BK, Weir B (eds) *Primer on Cerebrovascular Diseases*. Academic press, New York, pp 93-6, 1997.

Busija, D. W. Nervous control of the cerebral circulation. In: T. Bennett and S. M. Gardiner (eds) *Nervous Control of the Circulation*. Harwood Academic Publishers, Amsterdam, pp 177-206, 1996.

Busija, D. W., and C. Thore. Modulation of prostaglandin production by nitric oxide in astroglia. *Prost. Leuk. Fatty Acids.* 56:355-9, 1997.

Busija, D. W., and W. Meng. Altered cerebrovascular responsiveness to N-methyl-D-aspartate after asphyxia in piglets. *Am. J. Physiol.* 265:H389-94, 1993.

Chemtob, S., K. Beharry, J. Rex, T. Chatterjee, D. R. Varma, and J. V. Aranda. Ibuprofen enhances retinal and choroidal blood flow autoregulation in newborn piglets. *Invest. Ophthalmol.* 32:1799-807, 1991.

Chemtob, S., M. S. Roy, D. Abran, H. Fernandez, D. R. Varma. Prevention of postasphyxial increase in lipid peroxides and retinal function deterioration in the newborn pig by inhibition of cyclooxygenase activity and free radical generation. *Pediatric Res.* 33:336-40, 1993.

Choi, D.W. The Excitotoxic Concept in: *Primer on Cerebrovascular Diseases* eds.: Welch KMA, Caplan LR, Reis DJ, Siesjö BoK, Weir B, Academic Press, New York, 187-9, 1997.

Curtis, J. F., N. G. Reddy, R. P. Mason, B. Kalyanaraman, and T. E. Eling. Nitric oxide: a prostaglandin H synthase 1 and 2 reducing cosubstrate that does not stimulate cyclooxygenase activity or prostaglandin H synthase expression in murine macrophages. *Arch. Biochem. Biophys.* 335:369-76, 1996.

DeWitt, D. L. Prostaglandin endoperoxide synthase: regulation of enzyme expression. *Biochem. Biophys. Acta.* 1083:121-34, 1991.

Domoki, F., R. Veltkamp, N. Thrikawala, G. Robins, F. Bari, T. M. Louis, and D. W. Busija. Ischemia-reperfusion rapidly increases COX-2 expression in piglet cerebral arteries. *Am. J. Physiol.* 277:H1207-14, 1999.

Dumont, I., K.G. Peri, P. Hardy, X. Hou, A.K. Martinez-Bermudez, S. Molotchnikoff, D.R. Varma, and S. Chemtob. PGE<sub>2</sub>, via EP<sub>3</sub> receptors, regulates brain nitric oxide synthase in the perinatal period. *Am. J. Physiol.* 275:R1812-21, 1998.

Floyd, R.A. Production of Free Radicals in: *Primer on Cerebrovascular Diseases* eds.: Welch KMA, Caplan LR, Reis DJ, Siesjö BoK, Weir B, Academic Press, New York, 165-9, 1997.

Frick, K. K., L. Jiang, and D. A. Bushinsky. Acute metabolic acidosis inhibits the induction of osteoblastic egr-1 and type 1 collagen. *Am. J. Physiol.* 272:C1450-60, 1997.

Gass, P., C. Sommer, and M. Kiessling. Immediate-Early Gene Expression after Global Cerebral Ischemia and Ischemia Tolerance Induction in: *Primer on Cerebrovascular Diseases* eds.: Welch KMA, Caplan LR, Reis DJ, Siesjö BoK, Weir B, Academic Press, New York, 230-3, 1997.

Goh, Y., Y. Urade, N. Fujimoto, O. Hayaishi. Content and formation of prostaglandins and distribution of prostaglandin-related enzyme activities in the rat ocular system. *Biochim. Biophys. Acta.* 921:302-11, 1987.

Habib, A., C. Bernard, M. Lebret, C. Creminon, B. Esposito, A. Tedgui, and J. Maclouf. Regulation of the expression of cyclooxygenase-2 by nitric oxide in rat peritoneal macrophages. *J. Immunol.* 158:3845-51, 1997.

Hall, E.D. Lipid Peroxidation in: *Primer on Cerebrovascular Diseases* eds.: Welch KMA, Caplan LR, Reis DJ, Siesjö BoK, Weir B, Academic Press, New York, 200-4, 1997.

Hanna, N., K. G. Peri, D. Abran, P. Hardy, A. Doke, P. Lachapelle, M. S. Roy, J. Orquin, D. R. Varma, and S. Chemtob. Light induces peroxidation in retina by activating prostaglandin G/H synthase. *Free Rad. Biol. Med.* 23:885-97, 1997.

Hansen, A.J. Effect of anoxia on ion distribution in the brain. *Physiol. Rev.* 65:101-48, 1985.

Hara, K., D.L. Kong, F.R. Sharp, and P.R. Weinstein. Effect of selective inhibition of cyclooxygenase 2 on temporary focal cerebral ischemia in rats. *Neurosci. Lett.* 256:53-6, 1998.

Hardy, P., D. Abran, D. Y. Li, H. Fernandez, D. R. Varma, and S. Chemtob. Free radicals in retinal and choroidal blood flow autoregulation in the piglet: interaction with prostaglandins. *Invest. Ophthalmol.* 35:580-91, 1994.

Hardy, P., I. Dumont, M. Bhattacharya, X. Hou, P. Lachapelle, D.R. Varma, and S. Chemtob. Oxidants, nitric oxide and prostanoids in the developing ocular vasculature: a basis for ischemic retinopathy. *Cardiovasc. Res.* 47: 489-509. 2000

Hardy, P., M. Bhatthacharya, D. Abran, K. G. Peri, P. Asselin, D. R. Varma, and S. Chemtob. Increases in retinovascular prostaglandin receptor functions by cyclooxygenase- 1 and -2 inhibition. *Invest. Ophthalmol.* 39:1888-98, 1998.

Hayaishi, O. Sleep-wake regulation by prostaglandins D2 and E2. *J. Biol. Chem.* 263:14593-6, 1988.

Hossmann, K.A. The hypoxic brain. Insights from ischemia research. *Adv. Exp. Med. Biol.* 474:155-69, 1999.

Huang, P. L., Z. Huang, H. Mashimo, K. D. Bloch, M. A. Moskowitz, and M. C. Fishman. Effects of cerebral ischemia in mice deficient in neuronal nitric oxide synthase. *Science*. 265:1883-5, 1994.

Katsura, K., T. Kristian, M. L. Smith, and B. K. Siesjö. Acidosis induced by hypercapnia exaggerates ischemic brain damage. *J. Cereb. Blood Flow Metab.* 14:243-50, 1994.

Kaufmann, W. E., P. F. Worley, J. Pegg, M. Bremer, and P. Isakson. COX-2, a synaptically induced enzyme, is expressed by excitatory neurons at postsynaptic sites in rat cerebral cortex. *Proc. Natl. Acad. Sci. USA*. 93:2317-21, 1996.

Koistinaho, J., and T. Hökfelt . Altered gene expression in brain ischemia. *Neuroreport* 8:i-viii, 1997.

Kulkami, P., and S. Payne. Eicosanoids in bovine retinal microcirculation. *J. Ocul. Pharmacol. Ther.* 13:139-49, 1997.

Leffler, C. W., R. Mirro, W. M. Armstead, and D. W. Busija. Prostanoid synthesis and vascular responses to exogenous arachidonic acid following cerebral ischemia in piglets. *Prostaglandins*. 40:241-8, 1990.

Long, S. D., and P. H. Pekala. Regulation of GLUT4 gene expression by arachidonic acid: evidence for multiple pathways, one of which requires oxidation to prostaglandin E<sub>2</sub>. *J. Biol. Chem.* 271:1138-44, 1996.

MacRitchie, A.N., S.S. Jun, Z. Chen, Z. German, I.S. Yuhanna, T.S. Sherman, and P.W. Shaul. Estrogens upregulates endothelial nitric oxide synthase gene expression in fetal pulmonary artery endothelium. *Circ. Res.* 81:355-62, 1997.

Markrigrannakis, A. E., E. Zoumakis, A. N. Margioris, C. Stournaras, G. P. Chousos, and A. Gravanis. Regulation of the promoter of the human corticotropin-releasing hormone gene in transfected human endometrial cells. *Neuroendocrinology*. 64:85-92, 1996.

Matsuo, T., and M. S. Cynader. Localization of prostaglandin F<sub>2</sub> alpha and E<sub>2</sub> binding sites in the human eye. *Br. J. Ophthalmol.* 76:210-3, 1992.

Mirro, R., W. M. Armstead, D. W. Busija, and C. W. Leffler. Blood induced superoxide anion generation on the cerebral cortex of newborn pigs. *Am. J. Physiol.* 257:H1560-4, 1989.

Mishra, O.P., and M. Delivoria-Papadopoulos. Cellular mechanisms of hypoxic injury in the developing brain. *Brain Res. Bull.* 48:233-8, 1999.

Morimoto, Y., T. Yamamura, and O. Kemmotsu. Influence of hypoxic and hypercapnic acidosis on brain water content after forebrain ischemia in the rat. *Crit. Care Med.* 21:907-13, 1993.

Nogawa, S., F. Zhang, M. E. Ross, and C. Iadecola. Cyclo-oxygenase-2 gene expression in neurons contributes to ischemic brain damage. *J. Neurosci.* 17:2746-55, 1997.

O'Banion, M.K., V.D. Winn, and D.A. cDNA cloning and functional activity of a glucocorticoid-regulated inflammatory cyclooxygenase. *Proc. Natl. Acad. Sci. USA*. 89:4888-92, 1992

Parfenova, H., T. H. Eidson, and C. W. Leffler. Upregulation of COX-2 in cerebral microvascular endothelial cells by smooth muscle cell signals. *Am. J. Physiol.* 273:C277-88, 1997.

Peri, K. G., P. Hardy, D. Y. Li, D. R. Varma, and S. Chemtob. Prostaglandin G/H synthase-2 is a major contributor of brain prostaglandins in the newborn. *J. Biol. Chem.* 270:24615-20, 1995.

Pourcyrous, M., C. W. Leffler, H. S. Bada, S. B. Korones, and D. W. Busija. Brain superoxide anion generation in asphyxiated piglets and the effect of indomethacin at therapeutic dose. *Pediatric Res.* 34:366-9, 1993.

Raju, T.N. Some animal models for the study of perinatal asphyxia. *Biol. Neonate* 62:202-14, 1992.

Rothman, S.M, and J. W. Olney . Glutamate and the pathophysiology of hypoxic--ischemic brain damage. *Ann. Neurol.* 19:105-11. 1986

Salvemini, D., T. P. Misko, J. L. Masferrer, K. Seibert, M. G. Currie, and P. Needleman. Nitric oxide activates cyclooxygenase enzymes. *Proc. Natl. Acad. Sci. USA.* 90:7240-4, 1993.

Schmedtje Jr., J. F., Y. S. Ji, W. L. Liu, R. N. DuBois, and M. S. Runge. Hypoxia induces cyclooxygenase-2 via the NF-kappaB p65 transcription factor in human vascular endothelial cells. *J. Biol. Chem.* 272:601-8, 1997.

Sen, C. K., and L. Packer. Antioxidant and redox regulation of gene transcription. *FASEB J.* 10:709-20, 1996.

Shimizu, T., and L. S. Wolfe. Arachidonic acid cascade and signal transduction. *J. Neurochem.* 55:1-15, 1990.

Siesjö, B.K., and P. Siesjö. Mechanisms of secondary brain injury. *Eur. J. Anaesthesiol.* 13:247-68, 1996.

Smith, W. L. Prostanoid biosynthesis and mechanisms of action. *Am. J. Physiol.* 263:F181-91, 1992.

Stadler, J., B. G. Harbrecht, M. Di Silvio, R. D. Curran, M. L. Jordan, R. L. Simmons, and T. R. Billiar. Endogenous nitric oxide inhibits the synthesis of cyclooxygenase products and interleukin-6 by rat Kupffer cells. *J. Leukoc. Biol.* 53:165-72, 1993.

Stitt, J. T. Prostaglandin E as the neural mediator of the febrile response. *Yale J. Biol. Med.* 59:137-49, 1986.

Szabó, Cs. Physiological and pathophysiological roles of nitric oxide in the central nervous system. *Brain Res. Bull.* 41:131-41, 1996.

Thore, C. R., T. C. Beasley, and D. W. Busija. In vitro and in vivo localization of prostaglandin H synthase in fetal sheep neurons. *Neurosci. Lett.* 242:29-32, 1998.

Tsubokura, S., Y. Watanabe, H. Ehara, K. Imamura, O. Sugimoto, H. Kagamiyama, S. Yamamoto, and O. Hayaishi. Localization of prostaglandin endoperoxide synthase in neurons and glia in monkey brain. *Brain Res.* 543:15-24, 1991.

Vane, J.R., and R.M. Botting Pharmacodynamic profile of prostacyclin. *Am. J. Cardiol.* 75:3A-10A, 1995.

Vannucci, R. C. Perinatal hypoxic/ischemic encephalopathy. *Neurologist.* 1:35-52, 1995.

Vannucci, R. C., J. Towfighi, D. F. Heitjan, and R. M. Brucklacher. Carbon dioxide protects the perinatal brain from hypoxic-ischemic damage: an experimental study in the immature rat. *Pediatrics.* 95:868-74, 1995.

Vannucci, R. C. Mechanisms of perinatal hypoxic-ischemic brain damage. *Semin. Perinatol.* 17: 330-7, 1993.

Volpe, J. J. Brain injury in the premature infant--current concepts. *Prev. Med.* 23:638-45, 1994.

Wieloch, T.W., B. Hu, and M. Schamloo. Aberrant Cell Signaling in the Postischemic Brain: An Integrated View in: *Primer on Cerebrovascular Diseases* eds.: Welch KMA, Caplan LR, Reis DJ, Siesjö BoK, Weir B, Academic Press, New York, 227-9, 1997.

Williams, C. E., A. J. Gunn, C. Mallard, and P. D. Gluckman. Outcome after ischemia in the developing sheep brain: an electroencephalographic and histological study. *Ann. Neurol.* 31:14-21, 1992.

Wu, K. K. Cyclooxygenase 2 induction: molecular mechanism and pathophysiologic roles. *J. Lab. Clin. Med.* 128:242-5, 1996.

Yamagata, K., K. I. Andreasson, W. E. Kaufmann, C. A. Barnes, and P. F. Worley. Expression of a mitogen-inducible cyclooxygenase in brain neurons: regulation by synaptic activity and glucocorticoids. *Neuron*. 11:371-86, 1993.

Yamaji, Y., O. W. Moe, R. T. Miller, and R. J. Alpern. Acid activation of immediate early genes in renal epithelial cells. *J. Clin. Invest.* 94:1297-1303, 1994.

Zhang, Z. G., D. Reif, J. Macdonald, W. X. Tang, D. K. Kamp, R. J. Gentile, W. C. Shakespeare, R. J. Murray, and M. Chopp. ARL 17477, a potent and selective neuronal NOS inhibitor, decreases infarct volume after transient middle cerebral artery occlusion in rats. *J. Cereb. Blood Flow Metab.* 16:599-604, 1996.

Zhu, Y., T. S. Park, and J. M. Gidday. Mechanisms of hyperoxia-induced reductions in retinal blood flow in newborn pig. *Exp. Eye Res.* 67:357-69, 1998.

## Appendix

### Publications related to the subject of the thesis

- I. Dégi R, Bari F, Beasley TC, Thrikawala N, Thore C, Louis TM, Busija DW. (1998) Regional distribution of prostaglandin H synthase-2 and neuronal nitric oxide synthase in piglet brain. *Pediatr. Res.* 43: 683-9.
- II. Dégi R, Bari F, Thrikawala N, Beasley TC, Thore C, Louis TM, Busija DW. (1998) Effects of anoxic stress on prostaglandin H synthase isoforms in piglet brain. *Dev. Brain Res.* 107: 265-76.
- III. Dégi R, Thore C, Bari F, Thrikawala N, Robins G, Nógrádi A, Domoki F, Beasley TC, Busija DW (2001) Ischemia increases prostaglandin H synthase-2 levels in retina and visual cortex in piglets. *Graefe's Arch. Clin. Exp. Ophthalmol.* 239:59-65.
- IV. Busija, D. W., F. Bari, R. Dégi, F. Domoki, R. Veltkamp, T. M. Louis, N. Thrikawala, G. Robins (1998) Pathophysiology of COX-2 and NOS-derived metabolites and free radicals during brain ischemia. in *Pharmacology of cerebral ischemia* ed. J. Kriglstein pp.237-241. Medpharm, Stuttgart

### Additional publications:

1. Farkas G, Dégi R, Vörös P. (1995) Long-term effects of fetal islet transplantation on complication of diabetes, as compared with effects of intensive insulin therapy. *Transplant Proc* 27: 3145.
2. Vörös P, Farkas G, Lengyel Z, Dégi R, Rosivall L, Kammerer L. (1998) Albuminuria after fetal pancreatic islet transplantation: a 10-year follow-up. *Nephrol. Dial. Transplant* 13: 2899-904.
3. Sweatt AJ, Dégi R, Davis RM. (1999) Corneal wound-associated glycoconjugates analyzed by lectin histochemistry. *Curr Eye Res* 19:212-8.